International Geology Review

ISSN: (Print) (Online) Journal homepage: https://www.tandfonline.com/loi/tigr20

New ages from the Shackleton Glacier area and their context in the regional tectonomagmatic evolution of the Ross orogen of Antarctica

Timothy Paulsen , John Encarnación , Anne M. Grunow , Victor A. Valencia , Mark E. Pecha , Jeffrey Benowitz & Paul Layer

To cite this article: Timothy Paulsen , John Encarnación , Anne M. Grunow , Victor A. Valencia , Mark E. Pecha , Jeffrey Benowitz & Paul Layer (2020): New ages from the Shackleton Glacier area and their context in the regional tectonomagmatic evolution of the Ross orogen of Antarctica, International Geology Review, DOI: 10.1080/00206814.2020.1786737

To link to this article: https://doi.org/10.1080/00206814.2020.1786737

INTERNATIONAL GEOLOGY REVIEW
https://doi.org/10.1080/00206814.2020.1786737

Taylor & Francis
Taylor & Francis Group

ARTICLE

New ages from the Shackleton Glacier area and their context in the regional tectonomagmatic evolution of the Ross orogen of Antarctica

Timothy Paulsen[a], John Encarnación, Anne M. Grunow[b], Victor A. Valencia, Mark E. Pecha[c], Jeffrey Benowitz and Paul Layer

[a]Department of Geology, University of Wisconsin Oshkosh, Oshkosh, WI, USA; [b]Department of Earth and Atmospheric Sciences, Saint Louis University, St. Louis, MO, USA; [b]Byrd Polar Research Center, The Ohio State University, Columbus, OH, USA; [c]School of the Environment, Washington State University, Pullman, WA, USA; [c]Department of Geosciences, The University of Arizona, Tucson, AZ, USA; Geophysical Institute, University of Alaska Fairbanks, Fairbanks, AK, USA

ABSTRACT

The Ross orogenic belt in Antarctica is one of several Neoproterozoic-early Palaeozoic orogens that crisscrossed Gondwana and are associated with Gondwana's assembly. We present new age data from the Queen Maud Mountains, Ross orogen, from areas that hitherto have lacked precise ages from the local plutonic rocks. The zircon U-Pb igneous crystallization ages (n = 7) and a hornblende $^{40}Ar/^{39}Ar$ cooling age (n = 1) constrain plutonism to primarily lie within the Cambrian to Ordovician. Cumulative zircon U-Pb crystallization age data yield polymodal age distributions (516 Ma, 506–502 Ma, and 488 Ma age peaks) that are similar to other areas of the Queen Maud-Horlick Mountains, consistent with regional magmatic flare-ups along the Pacific-Gondwana margin during these times. The ages of deformed plutons constrain deformation to the Cambrian (Series 2) to Ordovician (Lower), with some regions indicating a transition to post-tectonic magmatism and cooling at ~509-470 Ma. Collectively, the data indicate that the Queen Maud-Horlick Mountains share a similar petrotectonic history with other regions of the Pacific-Gondwana margin, providing new evidence that this tectonostratigraphic province is part of and not exotic to the larger igneous-sedimentary successions developed in the peri-Gondwana realm under a broadly convergent margin setting.

ARTICLE HISTORY
Received 29 March 2020
Accepted 20 June 2020

KEYWORDS
Ross orogen; U-Pb geochronology; $^{40}Ar/^{39}Ar$ geochronology; Gondwana; Antarctica

1. Introduction

The late Neoproterozoic-early Palaeozoic assembly of Gondwana was marked by the development of several convergent margin-collisional orogens, including a major mountain belt along its paleo-Pacific convergent margin known as the Terra Australis orogen (Figure 1) (Grunow *et al*. 1996; Cawood 2005; Boger 2011). Exposures of the eroded remnants of these mountains in Antarctica and Australia are known as the Ross and Delamerian orogenic belts, respectively. The temporal and spatial patterns of magmatism and deformation within the Ross and Delamerian orogenic belts assume regional significance for the potential information they hold about the assembly of Gondwana (Stump 1992; Goodge *et al*. 1993a, 2002, 2004a, 2004b, 2012; Encarnación and Grunow 1996; Grunow *et al*. 1996; Goodge 1997, 2020; Cawood 2005; Stump*et al*. 2006; Boger 2011; González *et al*. 2018), an important time period marked by a radiative explosion of life and several extinction events (Squire *et al*. 2006; McKenzie *et al*. 2014). In Antarctica, geoscientists have long been working to date the age of magmatism and deformation within the Ross orogen (Laird 1991). However, our understanding of the ages of magmatism and deformation remains at a reconnaissance level for many regions because of the difficulties surrounding the study of these remote areas of the Earth. This paper presents and examines new U-Pb zircon and $^{40}Ar/^{39}Ar$ isotopic data from the Shackleton Glacier region of the Queen Maud Mountains, a region where relatively undeformed and unmetamorphosed intrusives, carbonates, clastics, and volcanics as well as their deformed/metamorphosed equivalents are excellently exposed. Although several ages for supracrustal units are available for these areas, significant exposures of plutonic rock in these same areas, including potential East Antarctic cratonic rock, have not been dated despite the fact that such data hold important information about the tectonomagmatic evolution of Gondwana's paleo-Pacific margin.

CONTACT Timothy Paulsen, paulsen@uwosh.edu Department of Geology, University of Wisconsin Oshkosh., Oshkosh, WI 54901, USA
The supplementary data for this article from can be access here.

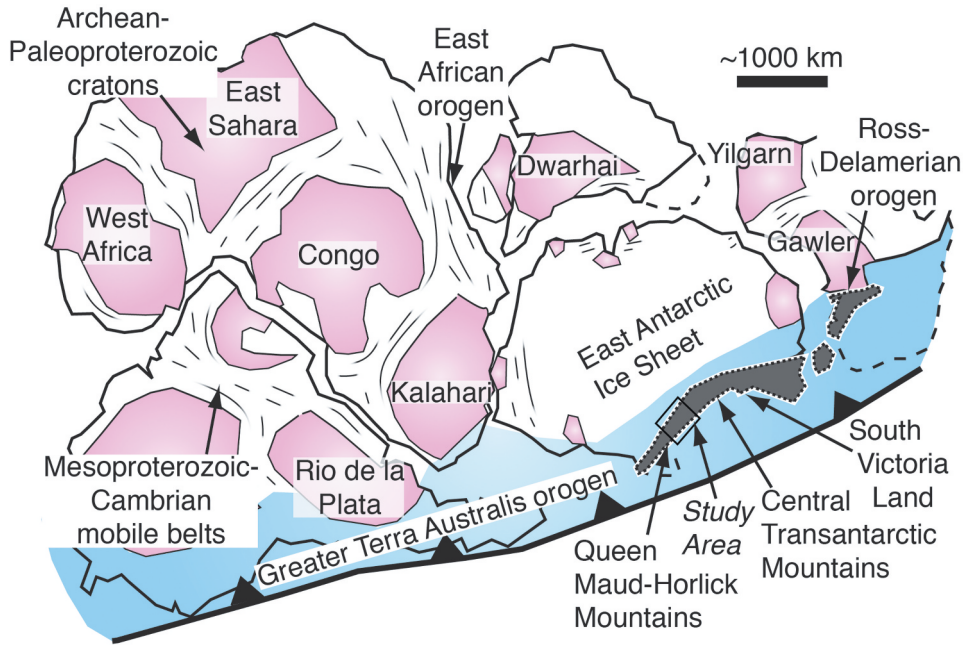

Figure 1. Gondwana reconstruction showing the Ross-Delamerian orogen within the greater latest Neoproterozoic to late Palaeozoic Terra Australis orogen, as well as the major Precambrian cratons and mobile belts of Gondwana. Figure modified from Paulsen *et al*. (2016b).

Throughout this paper, we use the 2015 International Chronostratigraphic Chart time scale (Cohen *et al*. 2013).

2. Geology of the Queen Maud and Horlick mountains

The erosional remnants of the Ross orogenic belt are primarily found in the Transantarctic Mountains where they lie below the Kukri erosion surface, a regionally extensive unconformity that is overlain by relatively undeformed, horizontal Devonian-Jurassic sedimentary rocks of the Beacon Supergroup (Stump 1995; Goodge 2020). Stratigraphic successions below the unconformity belong to the Ross Supergroup, which has traditionally been divided into the Beardmore and Liv groups in the Queen Maud-Horlick Mountains. The Beardmore Group includes greenschist facies siliciclastic rocks belonging to the La Gorce, Duncan, and Party formations (Figure 2) (Laird *et al*. 1971; Stump 1981, 1982, 1995). The Liv Group in turn includes a varied assemblage of meta-rhyolitic, -basaltic, and -volcaniclastic rocks, limestones, argillites, and quartz-rich sandstones belonging to the Wyatt, Ackerman, Leverett, Taylor, Fairweather, and Greenlee formations (Figure 2) (Stump 1982, 1986, 1995; Rowell and Rees 1989; Rowell *et al*. 1997; Wareham *et al*. 2001). U-Pb detrital zircon analyses have yielded Neoproterozoic to Cambrian maximum depositional ages for the Beardmore Group, whereas palaeontological and isotopic studies have yielded Cambrian ages for sedimentary and volcanic rocks of the Liv Group (Encarnación and Grunow 1996; Rowell *et al*. 1997; Van Schmus *et al*. 1997; Encarnación *et al*. 1999; Paulsen *et al*. 2015, 2016c, 2017, 2018).

Chemical and isotopic signatures indicate that the bimodal (basaltic and rhyolitic) volcanic rocks of the Liv Group are primarily derived from asthenospheric magmas and crustal melts interpreted to have formed within an intra-arc or back-arc extensional basin (Wareham *et al*. 2001). The presence of volcanic rocks in the Liv Group and their paucity in the group's stratigraphic equivalent (Byrd Group) at inboard localities (closer to the East Antarctic craton) in the central Transantarctic Mountains have been attributed to the outboard presence of a volcanic arc (Laird 1981). Other authors have argued that the volcanic-sedimentary successions of the outboard stratigraphic belt (Liv Group) represent suspect terrane(s) (i.e., the Queen Maud terrane; Figure 2) accreted to the East Antarctic margin during the Ross orogeny (Rowell and Rees 1989). Available palaeomagnetic data do not require that the Queen Maud terrane was far travelled or exotic and allow for autochthonous scenarios (Grunow and Encarnación 2000a).

The Ross Supergroup serves as the country rock for a widespread suite of intrusions (i.e., Queen Maud batholith) emplaced during the Ross orogeny, which in the Queen Maud-Horlick Mountains ranges from granite to gabbro in composition (McGregor 1965; Murtaugh 1969;

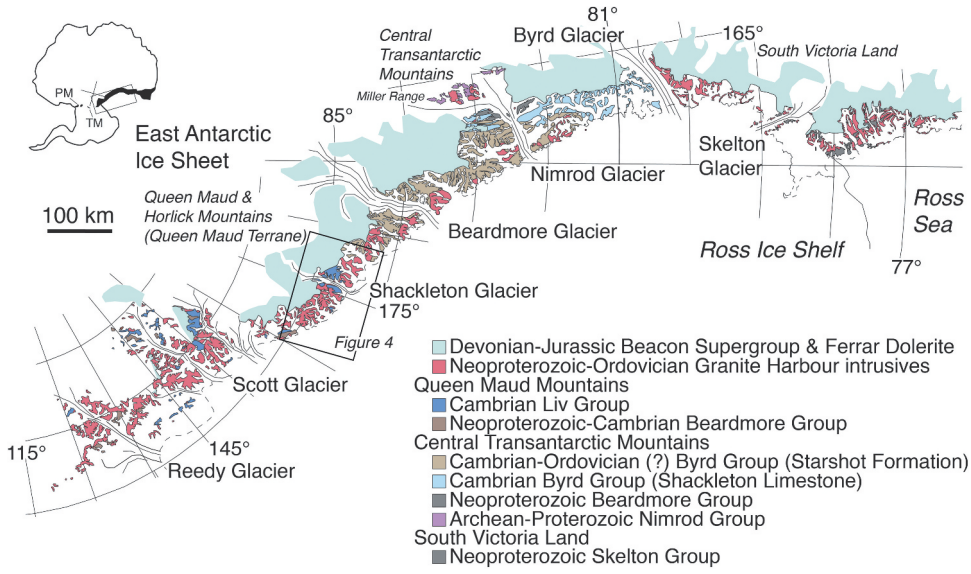

Figure 2. Simplified geologic map showing intrusive, sedimentary, and metamorphic basement rocks of the Ross orogen and unconformably overlying Beacon Supergroup from the central Transantarctic Mountains to the south through the Queen Maud and Horlick mountains. There are abundant volcanic rocks in early to middle Cambrian stratigraphic packages (i.e., the Liv Group) in the Queen Maud Mountains, whereas the early to middle Cambrian stratigraphic packages (i.e., the Byrd Group) in the central Transantarctic Mountains are practically devoid of volcanic rocks. The boundary separating the Liv Group from the Byrd Group occurs west of Shackleton Glacier. Inset shows location of the Transantarctic Mountains (~the black area is the Ross orogen). Abbreviations: PM, Pensacola Mountains; TM, Thiel Mountains. Figure compiled and modified from Grindley and McDougall (1969), McGregor and Wade (1969), Mirsky (1969), Warren (1969), and Davis and Blankenship (2005).

Borg *et al*. 1990; Stump 1995). Isotopic patterns of intrusive rocks indicate partial melting of mantle and Precambrian basement source rocks (Borg *et al*. 1990; Borg and DePaolo 1991, 1994). Early field investigations classified intrusions with secondary, solid-state foliations as being pretectonic to syntectonic in age, whereas intrusive bodies lacking such fabrics have been considered post-tectonic in age (McGregor 1965). Although early K-Ar and Rb-Sr geochronology suggested that some deformed igneous rocks of the Queen Maud batholith have Late Proterozoic emplacement ages (Felder and Faure 1979; Faure *et al*. 1979), recent zircon U-Pb geochronology indicates that the crystallization of igneous rocks primarily occurred ~535-490 Ma (Figure 3) (Encarnación and Grunow 1996; Van Schmus *et al*. 1997; Vogel *et al*. 2002; Paulsen *et al*. 2008, 2013, 2018). However, several exposures of deformed intrusive rocks and their metamorphic equivalents remain as candidates for Precambrian cratonic crust since the geology of many areas is only known at a reconnaissance level and there is a general lack of firm age control for crystalline rocks over large areas of the orogen. Establishing the ages and distributions of the various basement rocks bears on questions of concerning the spatio-temporal patterns of magmatism and deformation within orogenic belts during Gondwana assembly, as well as potentially providing key ages for cratonic crust that may constrain pre-Gondwanan continental reconstructions.

Despite recent progress towards understanding the geochronology of igneous rocks associated with the Queen Maud batholith, there are significant uncertainties about the timing of magmatism and deformation represented by undeformed and deformed intrusive rocks because of the limited number of age analyses and their limited clustering over the large area of the batholith. For example, apart from the five U-Pb crystallization ages (535–498 Ma) acquired from undeformed intrusive rocks (n = 3) and orthogneisses (n = 2) (Paulsen *et al*. 2013), there has been no other U-Pb zircon age investigation of these rock suites from over large areas of the Liv, Shackleton, and Ramsey glacier areas. In addition, only four $^{40}Ar/^{39}Ar$ cooling ages (500–484 Ma) have been reported for orthogneisses from this same region (Paulsen *et al*. 2004, 2013) and these cluster over a small area (two localities). Furthermore, no $^{40}Ar/^{39}Ar$ cooling ages have been reported for undeformed igneous rocks from this area. This paper focuses on filling the gap in knowledge about the ages of intrusive rocks of the Queen Maud Mountains through the presentation of new zircon U-Pb (n = 7) and hornblende and biotite $^{40}Ar/^{39}Ar$ (n = 2) age analyses of igneous plutonic rocks (four deformed and four undeformed intrusive rocks)

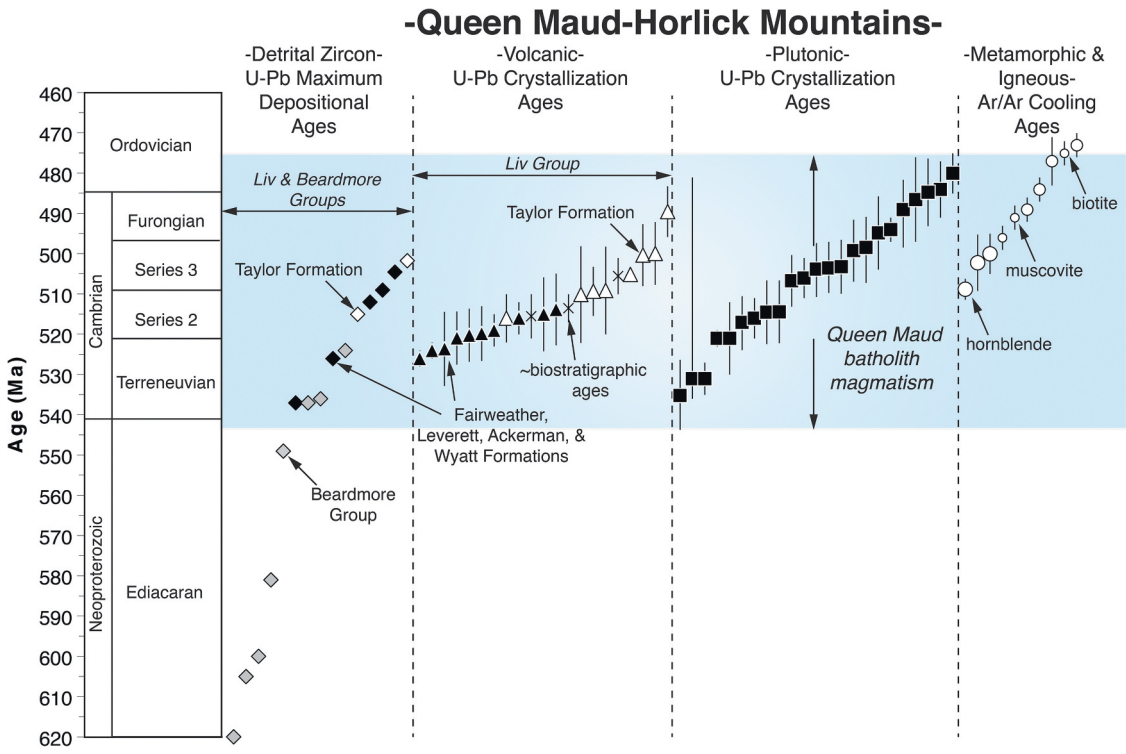

Figure 3. Diagram summarizing the available age constraints for the maximum depositional ages of siliciclastic rocks, crystallization ages of volcanic and plutonic rocks, and cooling ages of igneous and metamorphic rocks within the Queen Maud-Horlick Mountains sector of the Ross orogen. Gray symbols, Beardmore Group; black symbols, Fairweather, Leverett, Ackerman, and Wyatt formations; white symbols, Taylor Formation. Vertical black lines show errors on ages. Ages are compiled from Encarnación and Grunow (1996), Rowell *et al*. (1997), Van Schmus *et al*. (1997), Encarnación *et al*. (1999), Grunow and Encarnación (2000b), Vogel *et al*. (2002), Paulsen *et al*. (2004, 2008, 2013, 2015, 2017, 2018), and Stump *et al*. (2007).

from key localities in the broader Shackleton Glacier region (Figure 4), including seven samples acquired from the Polar Rock Repository (those with PRR numbers) and one from another collection. Our purpose is to better constrain the timing of magmatism and deformation in this important area and to consider their implications in the context of the regional tectonomagmatic evolution of the Ross orogen in Antarctica.

3. U-Pb methods

Zircon mineral concentrates were obtained from seven igneous plutonic (four deformed and three undeformed intrusive rocks) samples by conventional mineral separation techniques. A split of these grains (generally 50–100 grains) was selected from the grains available and incorporated into a 1" epoxy mount together with fragments of Sri Lanka and R33 standard zircons.

U-Pb geochronology of zircons was conducted by laser ablation multicollector inductively coupled plasma mass spectrometry (LA-MC-ICPMS) at the Arizona LaserChron Centre (Gehrels *et al*. 2008). The methods used for the analysis of zircons from samples 1228951 and WSH6B (PRR-16883) follow those applied to sample 12-8-95-2 described in Paulsen *et al*. (2013). The methods used for the analysis of zircons from the remaining five samples are described in detail by Gehrels *et al*. (2008), and thus it is only briefly described below. U-Pb analyses were conducted using a New Wave 193-nm laser coupled with a GVI Isoprobe multicollector ICP-MS. Laser ablation parameters used for this study employed laser spot size diameters of 35 μm, with a repetition rate of 10 Hz, and a few of ~4-5 J/cm^2. Each analysis consisted of one 12-s integration on peaks with the laser off (for backgrounds), 12 one-second integrations with the laser firing, and a 30 second delay to purge the previous sample and prepare for the next analysis.

For each analysis, the errors in determining $^{206}Pb/^{238}$ U and $^{206}Pb/^{204}Pb$ result in a measurement uncertainty of ~1-2% (at 1-sigma level) in the $^{206}Pb/^{238}$ U age. The errors in measurement of $^{206}Pb/^{207}Pb$ and $^{206}Pb/^{204}Pb$ also result in ~1-2% (at 1-sigma level) uncertainty in the $^{206}Pb/^{207}Pb$ age for grains that are >1000 Ma, but are substantially larger for younger grains due to low intensity of the ^{207}Pb signal. Interpreted ages are based on $^{206}Pb/^{238}$ U for <1000 Ma grains and on $^{206}Pb/^{207}Pb$ for >1000 Ma

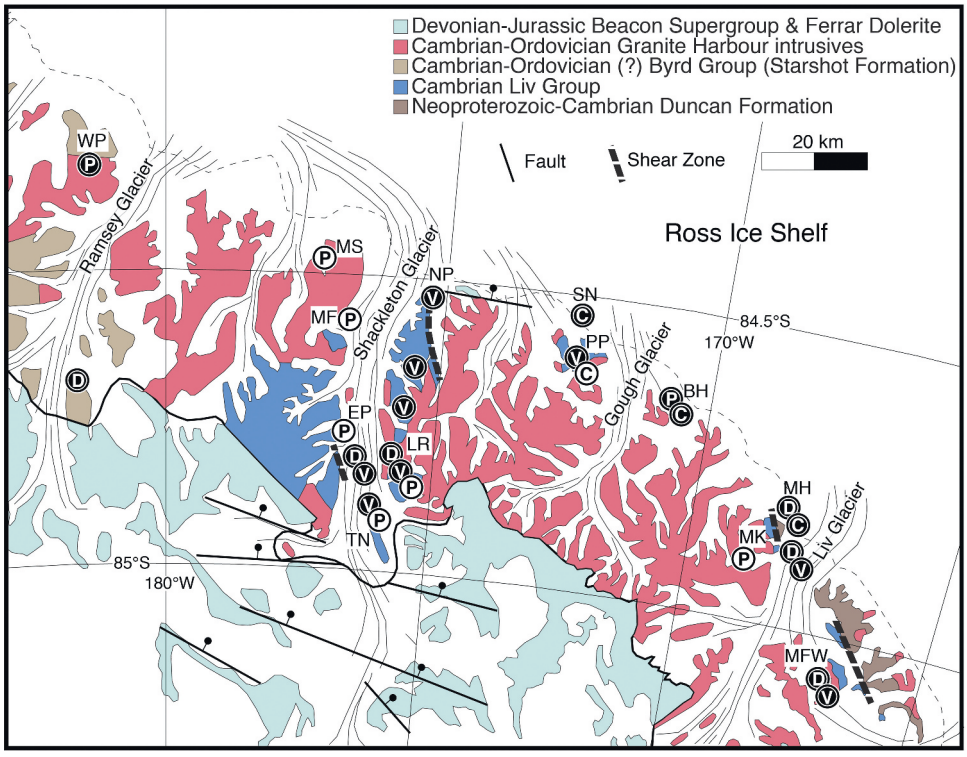

Figure 4. Simplified map showing the sample localities and geology in the Ramsey, Shackleton, and Liv glacier areas (modified from McGregor and Wade 1969). White circles show localities of plutonic rock samples analysed herein using U-Pb (P, plutonic) and $^{40}Ar/^{39}Ar$ (C, cooling) methods. Black circles show locations of previous U/Pb analyses of plutonic (P), volcanic (V), and siliciclastic (D) rocks, as well as previous $^{40}Ar/^{39}Ar$ analyses of plutonic and metasedimentary rocks (C) reported in Van Schmus *et al*. (1997), Encarnación *et al*. (1999), Paulsen *et al*. (2015, 2017, 2018). Curvilinear black line is location of unconformable contact between Ross Supergroup rocks and Beacon Supergroup. Abbreviations: BH, Bravo Hills; EP, Epidote Peak; LR, Lubbock Ridge; MF, Mount Franke; MH, Mount Henson; MFW, Mount Fairweather; MK, Mount Koob; MS, Mount Speed; PP, Polaris Peak; SN, Sage Nunataks; TN, Taylor Nunatak; WP, Woodall Peak.

grains. This division at 1000 Ma results from the increasing uncertainty of $^{206}Pb/^{238}$ U ages and the decreasing uncertainty of $^{206}Pb/^{207}Pb$ ages as a function of age.

Common Pb correction is accomplished by using the measured ^{204}Pb and assuming an initial Pb composition from Stacey and Kramers (1975) (with uncertainties of 1.0 for $^{206}Pb/^{204}Pb$ and 0.3 for $^{207}Pb/^{204}Pb$). Our measurement of ^{204}Pb is unaffected by the presence of ^{204}Hg because backgrounds are measured on peaks (thereby subtracting any background ^{204}Hg and ^{204}Pb), and because very little Hg is present in the argon gas.

Inter-element fractionation of Pb/U is generally ~20%, whereas apparent fractionation of Pb isotopes is generally ~2%. In-run analysis (one or two every fifth measurement) of fragments of a large zircon crystal with the known age of 564.2 ±3.2 Ma (2-sigma error, Gehrels *et al*. 2008) is used to correct for this fractionation. The measurement uncertainty resulting from the calibration correction is generally 1–2% (2-sigma) for both $^{206}Pb/^{207}Pb$ and $^{206}Pb/^{238}$ U ages. In the present study, analyses of quality control zircon R33 yielded a weighted mean age for $^{206}Pb/^{238}$ U of 418.3 ± 2.2 Ma (n = 20, MSWD = 0.6) compared to an ID-TIMS age of ~419 Ma (Black *et al*. 2004).

Concentrations of U and Th are calibrated relative to Sri Lanka zircon, which contains ~518 ppm of U and 68 ppm Th (Gehrels *et al*. 2008).

The analytical data are reported in Appendix A. Uncertainties shown in this table are at the 1-sigma level, and include only measurement errors.

The resulting interpreted ages are shown in Figure 5 on concordia diagrams and weighted mean diagrams using the routines in Isoplot (Ludwig 2008). The weighted mean diagrams show the weighted mean (weighting according to the square of the internal uncertainties) reported at 2-sigma, the uncertainty of the weighted mean, the external (systematic) uncertainty that corresponds to the ages used, the final uncertainty of the age (determined by quadratic addition of the weighted mean and external uncertainties), and the MSWD of the data set. The systematic error includes contributions from the standard calibration, age of the calibration standard, composition of common Pb, and U decay constants, and in this data set range from 1.2%

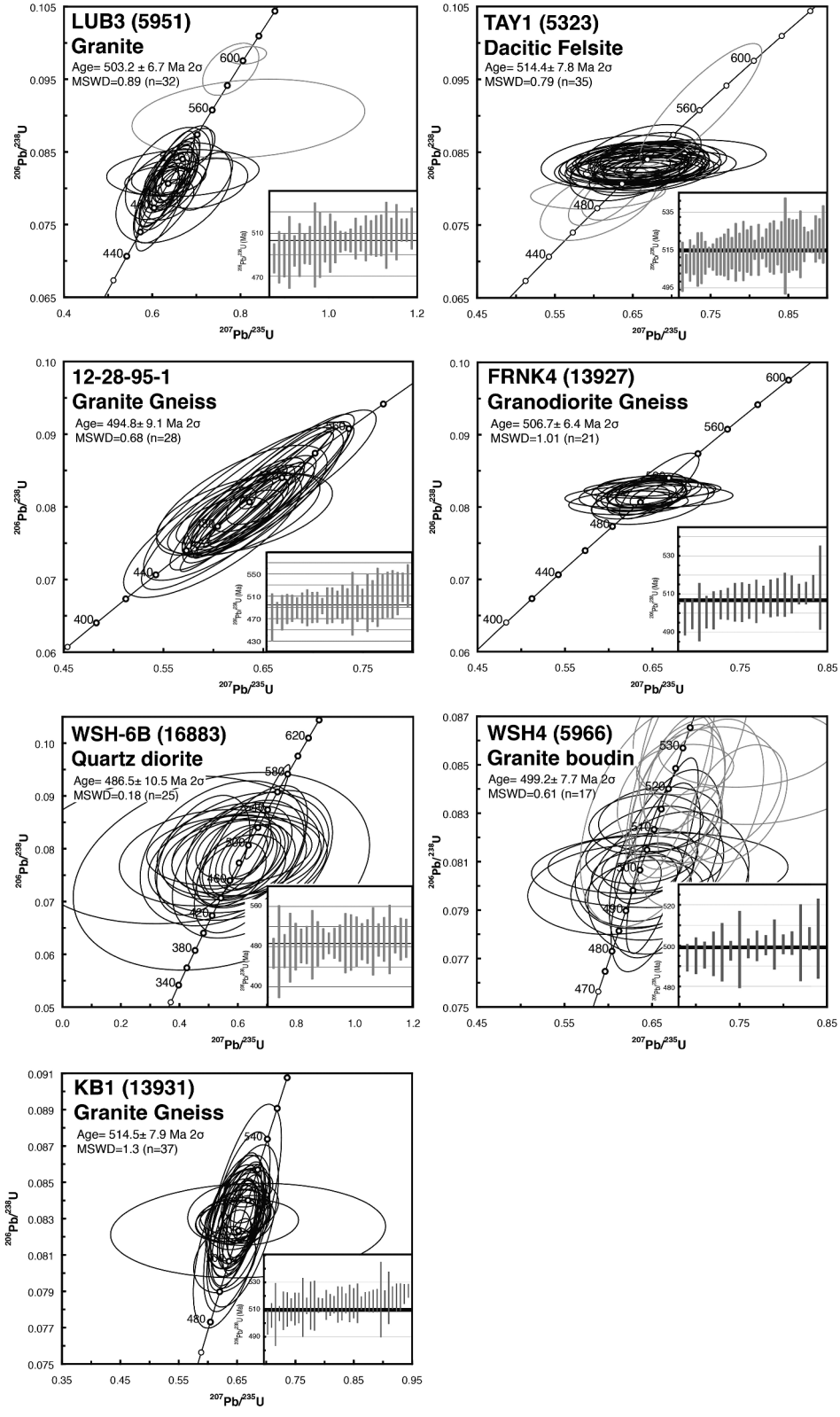

Figure 5. Concordia diagrams of zircon U-Pb data and weighted mean $^{206}Pb/^{238}$ U age plots of individual analyses for plutonic samples from the area of the Shackleton to Liv glaciers. Error bars in insets are 1-sigma. Data error ellipses are 2-sigma.

to 1.5% (2-sigma). The following presentation of the zircon U-Pb ages is separated by sample localities.

4. U-Pb results

4.1 Upper Shackleton Glacier

4.1.1 Lubbock Ridge

Sample LUB-3 (Polar Rock Repository sample PRR-5951) is an unfoliated intrusive rock collected by John Encarnación from the east end of Lubbock Ridge along the eastern flank of Shackleton Glacier where Stump (1986) mapped plutonic rocks that discordantly intrude deformed interbedded volcanic and siliciclastic rocks belonging to the Taylor Formation (Figure 4). The LUB-3 sample (Appendix B) is an unfoliated, medium- to coarse-grained, leucocratic, porphyritic, hornblende-biotite granite (Figures 6 and 7(a)). Quartz has no or weak undulatory extinction and lacks subgrains and feldspar is locally sericitized in patches. Zircons from the LUB-3 sample typically have prismatic euhedral shapes with well-developed oscillatory zoned interiors that in some cases rim unzoned and oscillatory zoned xenocrystic cores. All of the analysed zircon grains have magmatic U/Th ratios (0.6–2.9) (Rubatto 2002; Hoskin and Schaltegger 2003). U/Pb zircon analyses yield ages ranging from 604 to 477 Ma (Ediacaran-Ordovician). A coherent group of 32 of the 35 total analyses yield a weighted mean $^{206}Pb/^{238}$ U age of 503 ± 7 Ma considered to be the crystallization age for the sample (Figure 5). This age is broadly consistent with a 516 ± 6 Ma $^{206}Pb/^{238}$ U zircon crystallization age (Van Schmus *et al*. 1997) and a 515 Ma $^{206}Pb/^{238}$ U detrital zircon maximum depositional age (Paulsen *et al*. 2015, 2017) for the Taylor Formation country rock at this locality, as well as the field relations that indicate the Taylor Formation is older than the undeformed granite. The combination of these ages place deformation of the Taylor Formation to be within 522–496 Ma (Cambrian, Terreneuvian to Furongian) at this locality.

4.1.2 Taylor Nunatak

Sample TAY-I (PRR-5323) is an unfoliated intrusive rock collected by John Encarnación from the base of Taylor Nunatak along the eastern flank of Shackleton Glacier (Figure 4) where Stump (1986) mapped felsite stocks (Figure 8 (a,b)) that intrude deformed interbedded volcanic and sedimentary rocks belonging to the Taylor

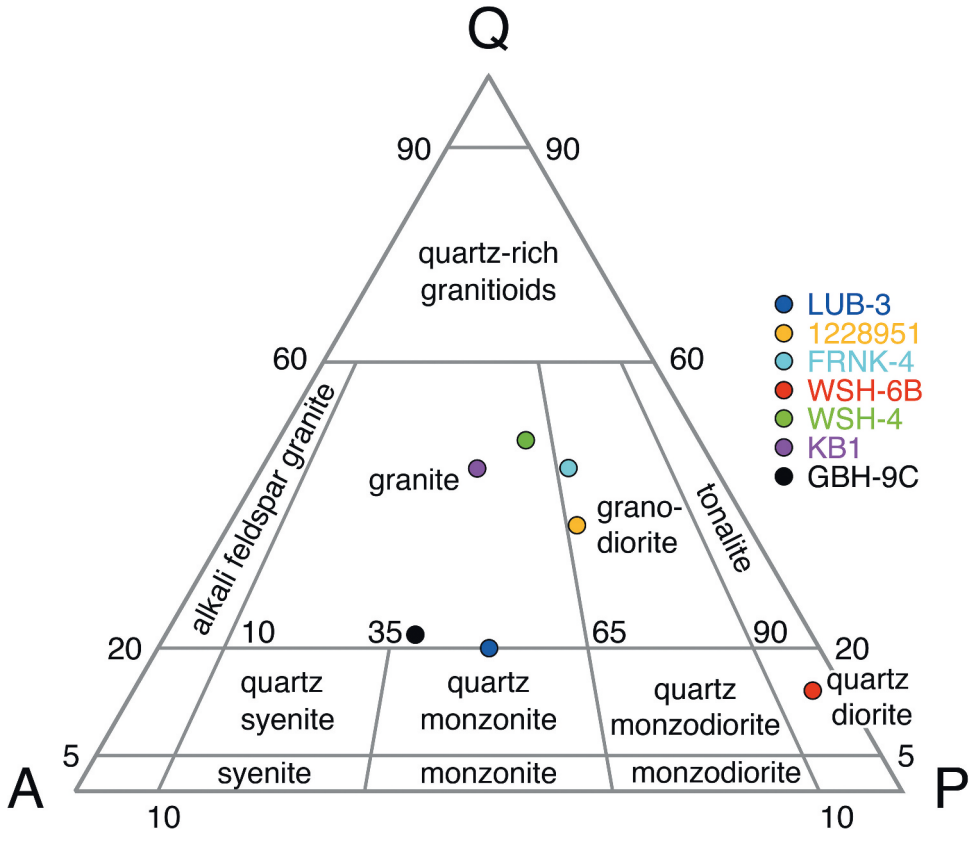

Figure 6. Ternary IUGS classification diagram of phaneritic plutonic samples based on modal analyses of mineralogy (Streckeisen 1974). Abbreviations: Q, quartz; A, alkali feldspar; P, plagioclase feldspar. Sample TAY-I is not plotted on account of its very fine-grained, aphanitic groundmass texture.

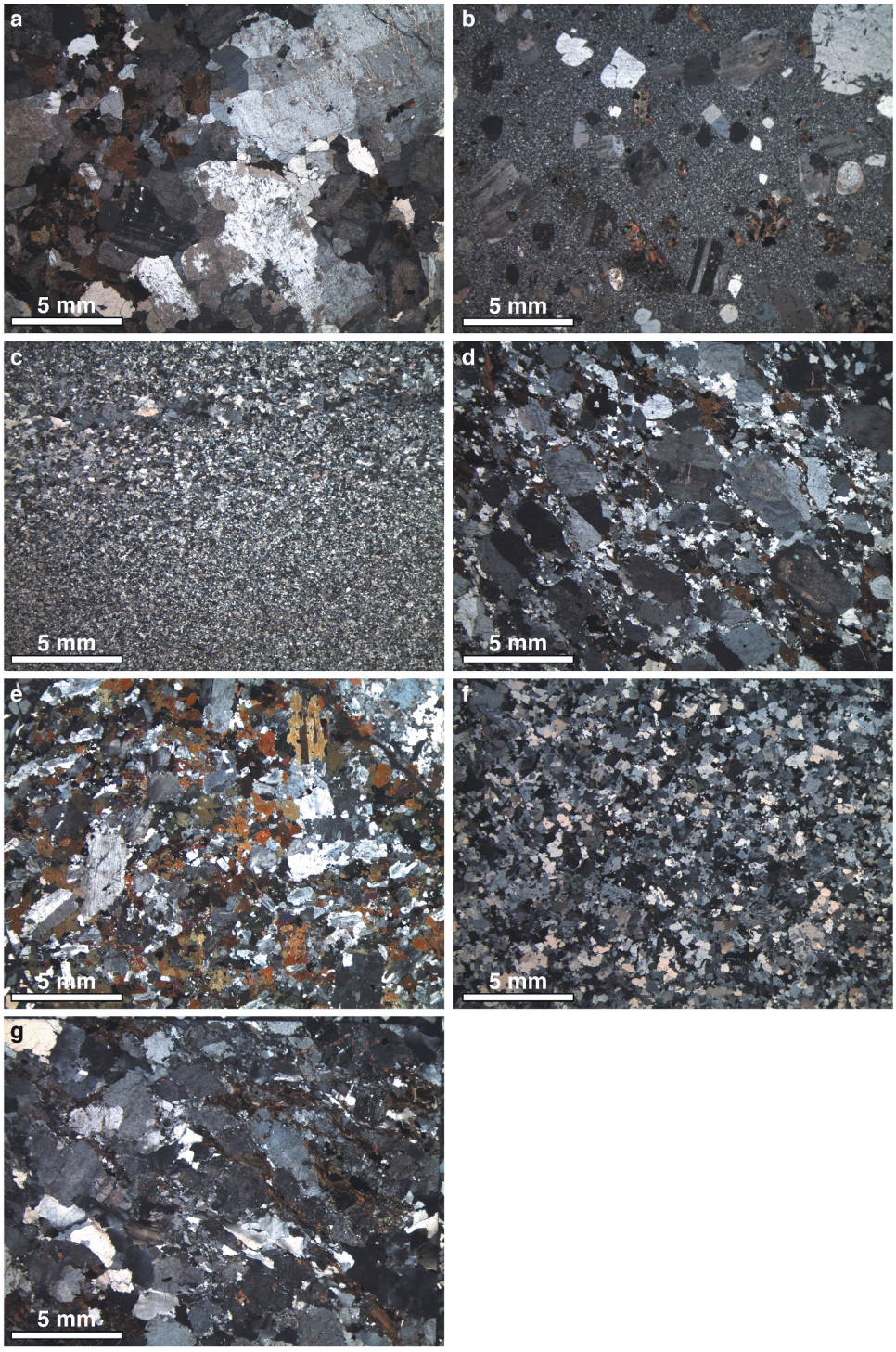

Figure 7. Photomicrographs of igneous samples analysed in this paper. (a) LUB-3 (PRR-5951) granite at Lubbock Ridge, (b) TAY-I (PRR-5323) dacitic felsite at Taylor Nunatak, (c) 1228951 granite gneiss (foliation subhorizontal in photomicrograph) at Epidote Peak, (d) FRNK-4 (PRR-13927) granodiorite gneiss (foliation upper left to lower right in photomicrograph) at Mount Franke, (e) WSH-6B (PRR-16883) quartz diorite at Mount Franke, (f) WSH-4 (PRR-5966) granite boudin at Mount Speed, and (g) KB1 (PRR-13931) granite gneiss (foliation upper left to lower right in photomicrograph) at Mount Koob.

Figure 8. (a) Aerial photo (TMA2189) of hypabyssal intrusive rocks (sample TAY-I) in the middle Cambrian Taylor Formation at Taylor Nunatak, (b) Photo of the unfoliated dacitic felsite stock at the TAY-I sample locality, (c) Photo of the east-dipping sedimentary-volcanic succession of the Taylor Formation at Taylor Nunatak, and (d) Photo of steeply-dipping, disjunctive pressure-solution cleavage within moderately-dipping limestone of the Taylor Formation at Taylor Nunatak.

Formation (Figure 8(c,d)). The TAY-I sample (Appendix B) is an unfoliated, quartz, pyroxene, and plagioclase phyric felsite (Figure 7(b)). Plagioclase, quartz, and pyroxene phenocrysts are suspended in a fine-grained xenomorphic granular groundmass of quartz and feldspar. Plagioclase shows patchy epidote and sericite alteration, quartz shows some resorption, and pyroxene phenocrysts are pseudomorphed by chlorite. While the groundmass is too fine-grained to accurately identify mineral abundances, phenocrysts are consistent with a dacitic composition. Zircons from the TAY-I sample have subhedral to euhedral shapes with well-developed oscillatory zoned interiors that in some cases rim xenocrystic cores. All of the analysed zircon grains have magmatic U/Th ratios (1.3–2.9) (Rubatto 2002; Hoskin and Schaltegger 2003). U/Pb zircon analyses yield ages ranging from 565 to 484 Ma (Ediacaran-Ordovician). A coherent group of 35 of 45 analyses yield a weighted mean $^{206}Pb/^{238}$ U age of 514 ± 8 Ma considered to be the crystallization age for the sample (Figure 5). This age is consistent with U-Pb dates and palaeontological (trilobite) data from deformed carbonate units (Cambrian, Series 3) interbedded with volcanic rocks (505 ± 1.5 Ma U-Pb crystallization age) at Taylor Nunatak (Encarnación *et al.* 1999), as well as the field relations that indicate the Taylor Formation is older than the undeformed felsite, given the uncertainties in the ages. The combination of the ages and their accompanying uncertainties with the relative ages from the field might narrowly constrain deformation of the Taylor Formation at ~506 Ma (Cambrian, Series 3) at this locality. An alternative and perhaps conservative minimum deformation age would be the 503 ± 7 Ma age from the undeformed cross-cutting granite (LUB-3) near Taylor Nunatak at Lubbock Ridge, which would constrain the youngest deformation of the Taylor Formation to be within 506.5–496 Ma (Cambrian, Series 3 to Furongian) at this locality.

4.1.3 Epidote Peak

Sample 1228951 is a foliated intrusive rock in the field and collected by Tim Paulsen from the base of Epidote Peak along the western flank of Shackleton Glacier (Figure 4) where Stump (1986) mapped migmatitic gneisses in contact with basal exposures of the Greenlee Formation (Figure 9). The 1228951 sample is a fine-grained, leucocratic, xenomorphic granular felsite (granite) gneiss (Figures 6 and 7(c)). The foliation is defined by alignment of amphiboles and bands of slightly coarser and finer quartzofeldspathic layers. Zircons from the 1228951 sample have anhedral to subhedral shapes with unzoned and oscillatory zoned interiors that in some cases rim xenocrystic cores. All of the analysed zircon grains have magmatic U/Th ratios (0.8–5.0) (Rubatto 2002; Hoskin and Schaltegger 2003).

U/Pb zircon analyses yield ages ranging from 579 to 446 Ma (Ediacaran-Ordovician). A coherent group of 28 of 34 analyses yield a weighted mean $^{206}Pb/^{238}$ U age of 495 ± 9 Ma considered to be the crystallization age for the sample (Figure 5) assuming the protolith is of igneous origin. If the protolith has a sedimentary component, then the 495 Ma weighted mean age is strictly a maximum depositional age. The nature of the protolith aside, the 495 ± 9 Ma weighted mean age places deformation of the 1228951 gneiss to be <504 Ma (Cambrian, Series 3), which is consistent with nearby sheared volcanic rocks of the Taylor and Greenlee formations that yield 510 ± 12 Ma to 500 ± 8 Ma U-Pb crystallization ages to the south at Mount Greenlee (Paulsen *et al*. 2018).

4.2 Lower Shackleton Glacier

4.2.1 Mount Franke

Sample FRNK-4 (PRR-13927) is a foliated intrusive rock collected by John Burgener from the northeast corner of Mount Franke on the western flank of Shackleton Glacier where Burgener (1975) reported orthogneisses (Figure 4) that are in turn crosscut by undeformed intrusions similar to the field relationships shown in (Figure 10(a)). The FRNK-4 sample (Appendix B) is a fine- to medium-grained, leucocratic, inequigranular hornblende-biotite granodiorite gneiss (Figures 6 and 7(d)). The foliation is defined by alignment of amphiboles and biotite with bands of quartz and felspar subgrains. Zircons from the FRNK-4 sample have anhedral to euhedral shapes with oscillatory-zoned interiors that in some cases rim unzoned and oscillatory zoned xenocrystic cores. All of the analysed zircon grains have magmatic U/Th ratios (1.7–5.3) (Rubatto 2002; Hoskin and Schaltegger 2003). U/Pb zircon analyses yield ages ranging from 521 to 481 Ma (Cambrian-Ordovician). A coherent group of 21 of 26 analyses yield a weighted mean $^{206}Pb/^{238}$ U age of 507 ± 7 Ma considered to be the crystallization age for the sample (Figure 5). The 507 ± 7 Ma crystallization age places deformation to be <514 Ma (Cambrian, Series 2), which is consistent with the crystallization age of sample WSH-6B described below.

Sample WSH-6B (PRR-16883) is an unfoliated intrusive rock collected by Anne Grunow from the base of the south side of Mount Franke on the western flank of Shackleton Glacier (Figure 4). The WSH-6B sample (Appendix B) is a seriate porphyritic, fine to coarse-grained, leucocratic, xenomorphic granular, biotite hornblende quartz diorite (Figures 6 and 7(e)). Although the WSH-6B sample shows no penetrative foliation/deformation, some plagioclase twins are bent and quartz grains locally show undulatory extinction and subgrain development suggesting it is a late to post-kinematic intrusive rock. Zircons from the WSH-6B sample have anhedral to subhedral shapes with unzoned and oscillatory zoned interiors that in some cases rim xenocrystic cores. All of the analysed zircon grains have magmatic U/Th ratios (0.6–6.1) (Rubatto 2002; Hoskin and Schaltegger 2003). U/Pb zircon analyses yield ages ranging from 538 Ma to 467 Ma (Cambrian-Ordovician). A coherent group of 25 of 26 analyses yield a weighted mean $^{206}Pb/^{238}$ U age of 486 ± 12 Ma considered to be the crystallization age for the sample (Figure 5). The combination of the FRNK-4 and WSH-6B crystallization ages place deformation recorded by the FRNK-4 gneiss to be within 514–474 Ma (Cambrian, Series 2 to Ordovician, Lower).

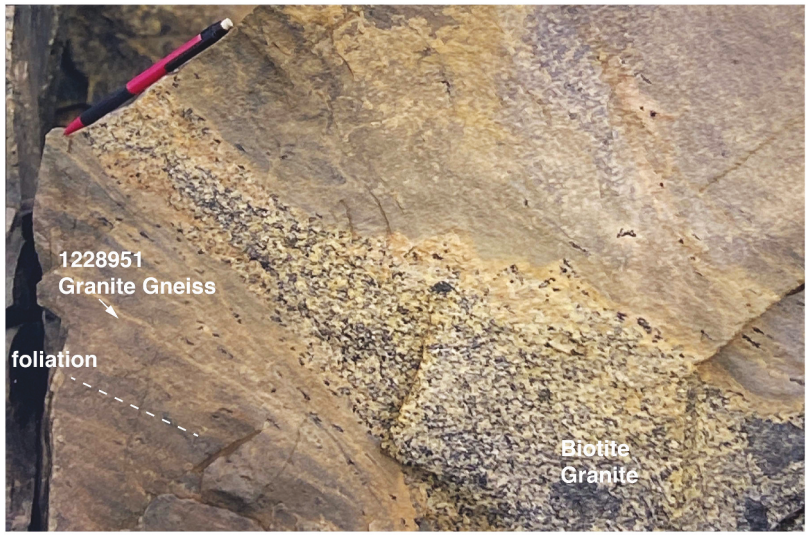

Figure 9. Photo of sample 1228951 granite gneiss at Epidote Peak with porphyroclasts of mafic rocks from a crudely foliated 'salt and pepper' biotite granite with which it is in contact.

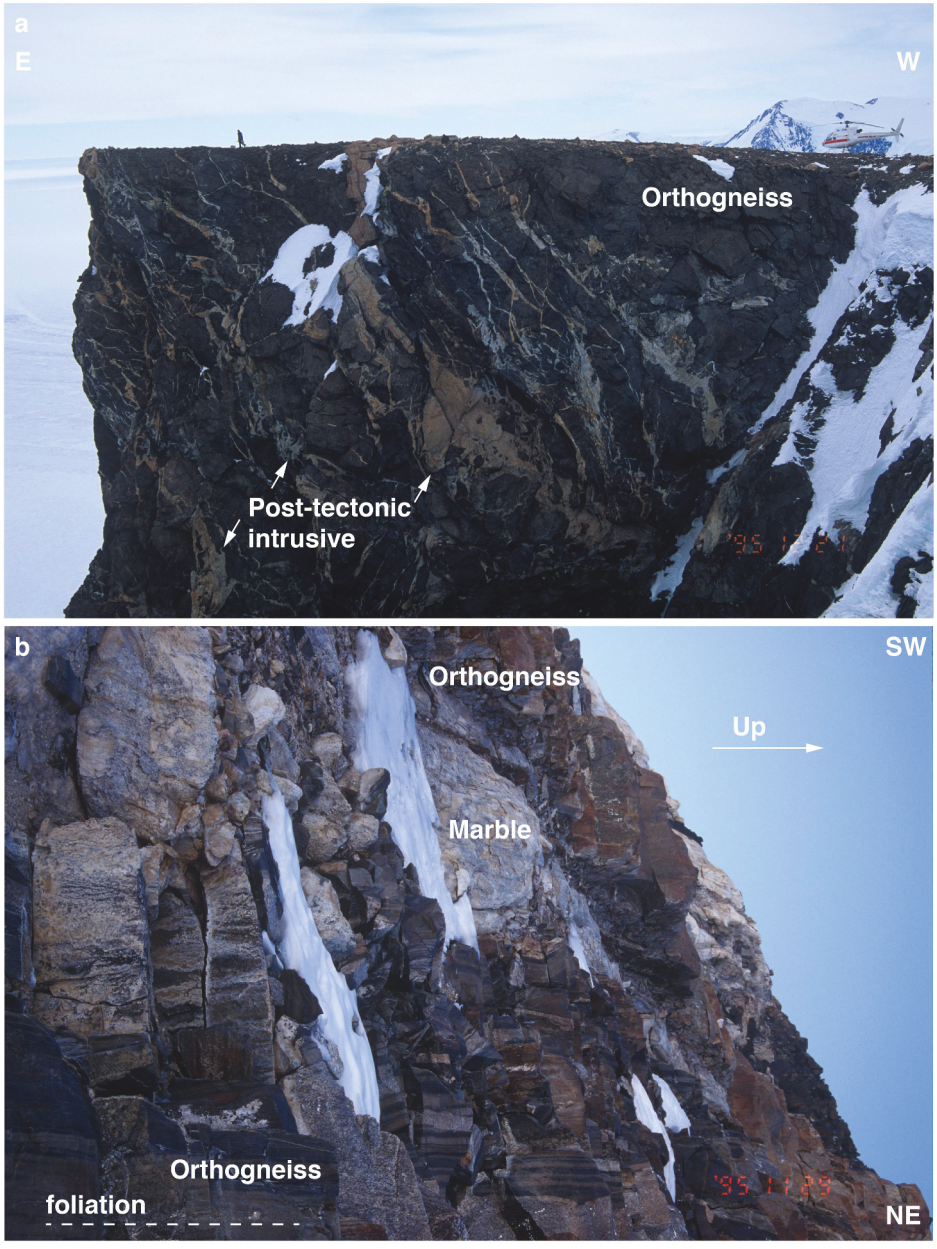

Figure 10. (a) Photo of orthogneiss (similar to FRNK-4 granodiorite gneiss) that hosts discordant undeformed intrusive rocks at Mount Franke, and (b) Photo of interleaved marbles and orthogneiss (similar to sample WSH-4 granite) at Mount Speed.

4.2.2 Mount Speed

Sample WSH-4 (PRR-5966) is an intrusive rock collected by John Encarnación from a northwest-trending spur north of Oppegaard Spur at the northwest corner of Mount Speed on the western side of Shackleton Glacier (Figure 4) near the locality where John Burgener described foliated tonalites in contact with marble and gabbro similar to the relationships shown in Figure 10(b) (Burgener 1975). Sample WSH-4 was collected from a boudin enclosed in coarse-grained white marble. Although the stratigraphic assignment of these marbles is unclear, they resemble descriptions of marbles that occur within the Taylor Formation at Mount Greenlee, Pallid Peak, and the western flank of Massam Glacier (Stump 1986; Wade and Cathey 1986). The WSH-4 sample (Appendix B) is a fine- to medium-grained, leucocratic, inequigranular, xenomorphic granular hornblende granite (Figures 6 and 7(f)). Alkali feldspar shows poikilitic and microperthitic textures and quartz displays subgrain development. Zircons from the WSH-4 sample have anhedral to subhedral shapes with unzoned and oscillatory zoned interiors that in some cases rim xenocrystic cores.

All of the analysed zircon grains have magmatic U/Th ratios (0.6–6.1) (Rubatto 2002; Hoskin and Schaltegger 2003). U/Pb zircon analyses yield ages ranging from 552 Ma to 477 Ma (Ediacaran-Ordovician). A coherent group of 17 of 35 analyses yield a weighted mean $^{206}Pb/^{238}$ U age of 499 ± 6 Ma considered to be the crystallization age for the sample (Figure 5). The 499 ± 6 Ma crystallization age places deformation recorded by the WSH-4 granite boudin to be <505 Ma (Cambrian, Series 3), which is consistent with deformation bracketed within 514–474 Ma (Cambrian, Series 2 to Ordovician, Lower) at Mount Franke. The 499 ± 6 Ma crystallization age also represents a minimum depositional age for the marble protoliths, which is consistent with U-Pb dates and palaeontological (trilobite) data that indicate a Cambrian, Series 2 to Series 3 depositional age for the Taylor Formation (Encarnación *et al*. 1999; Paulsen *et al*. 2015, 2017, 2018), possibly the unmetamorphosed equivalent of the marble.

4.3 Mount Henson Area

4.3.1 Mount Koob

Sample KB1 (PRR-13931) is a foliated intrusive rock collected by John Burgener from Mount Koob in the Mayer Crags region located ~8 km to the southwest of Mount Henson (Figure 4) (Burgener 1975). The KB1 sample (Appendix B) is a medium- to coarse-grained, leucocratic, inequigranular granite gneiss (Figures 6 and 7(g)). The foliation is defined by the alignment of elongate quartz, biotite, and feldspar, the latter of which show proto-augen morphologies. Zircons from the KB1 sample have anhedral to euhedral shapes with unzoned and oscillatory zoned interiors that in some cases rim xenocrystic cores. All of the analysed zircon grains have magmatic U/Th ratios (0.8–2.4) (Rubatto 2002; Hoskin and Schaltegger 2003). U/Pb zircon analyses yield ages ranging from 561 Ma to 491 Ma (Ediacaran-Ordovician). A coherent group of 37 of 48 analyses yield a weighted mean $^{206}Pb/^{238}$ U age of 515 ± 8 Ma (2 sigma) considered to be the igneous crystallization age for the protolith of the gneiss sample (Figure 5), which is similar to a 517 + 6.9/-6.5 Ma (2 sigma) igneous protolith crystallization age yielded by a diorite orthogneiss from the proximal area of the Bravo Hills. The subsolidus deformation fabric displayed by the KB1 granitic gneiss and its 515 ± 8 Ma igneous protolith crystallization age places deformation recorded by the KB1 gneiss to be <523 Ma (Cambrian, Terreneuvian), which is consistent with nearby deformation bracketed within 524–495 Ma (Cambrian, Terreneuvian to Furongian) in the Bravo Hills (Paulsen *et al*. 2013) and 509–472 Ma (Cambrian, Series 3 to Ordovician, Lower) at Mount Henson (Paulsen *et al*. 2004, 2015).

5. $^{40}Ar/^{39}Ar$ Methods

We analysed hornblende and biotite from an undeformed igneous plutonic sample (GBH-9C) in order to provide for the younger age-limit of deformation at Polaris Peak. The sample was submitted to the Geochronology Laboratory at University of Alaska Fairbanks for $^{40}Ar/^{39}Ar$ analysis where they were crushed, sieved, washed, and hand-picked for optically pure hornblende and biotite mineral phase separates. The monitor mineral MMhb-1 (Samson and Alexander 1987) with an age of 523.5 Ma (Renne 1994) was used to monitor neutron flux (and calculate the irradiation parameter, J). The samples and standard were wrapped in aluminium foil and loaded into aluminium cans of 2.5 cm diameter and 6 cm height. The samples were irradiated in position 5 c of the uranium enriched research reactor of McMaster University in Hamilton, Ontario, Canada for 20 megawatt-hours.

Upon return from the reactor, the samples and monitor were loaded into 2 mm diameter holes in a copper tray that was then loaded in a ultra-high vacuum extraction line. The monitor was fused, and samples heated, using a 6-watt argon-ion laser following the technique described in York *et al*. (1981), Layer *et al*. (1997), Layer (2000), and Benowitz *et al*. (2014). Argon purification was achieved using a liquid nitrogen cold trap and a SAES Zr/Al getter at 400 C. The samples were analysed in a VG-3600 mass spectrometer at the Geophysical Institute, University of Alaska Fairbanks. The argon isotopes measured were corrected for system blank and mass discrimination, as well as calcium, potassium, and chlorine interference reactions following procedures outlined in McDougall and Harrison (1991). Typical full-system 8 min laser blank values (in moles) were generally 2×10^{-16} mol ^{40}Ar, 3×10^{-18} mol ^{39}Ar, 9×10^{-18} mol ^{38}Ar and 2×10^{-18} mol ^{36}Ar, which are 10–50 times smaller than the sample/standard volume fractions. Correction factors for nucleogenic interferences during irradiation were determined from irradiated CaF_2 and K_2SO_4 as follows $(^{39}Ar/^{37}Ar)Ca = 7.06 \times 10^{-4}$, $(^{36}Ar/^{37}Ar)Ca = 2.79 \times 10^{-4}$ and $(^{40}Ar/^{39}Ar)K = 0.0297$. Mass discrimination was monitored by running calibrated air shots. The mass discrimination during these experiments was 1.3% per mass unit. While doing our experiments, calibration measurements were made on a weekly to monthly basis to check for changes in mass discrimination with no significant variation seen during these intervals.

The analytical data are reported in Appendix C. Uncertainties are calculated using the constants of

Renne *et al*. (2010) and shown in this table are at the 1-sigma level. The integrated age is the age given by the total gas measured and is equivalent to a potassium-argon (K-Ar) age. The spectrum provides a plateau age if three or more consecutive gas fractions represent at least 50% of the total gas release and are within two standard deviations of each other (Mean Square Weighted Deviation less than or equal to 2.5).

6. $^{40}Ar/^{39}Ar$ Results

Sample GBH-9C (PRR-5289) is an unfoliated intrusive rock collected by John Encarnación near Polaris Peak (Figure 4) where Stump (1986) mapped the GBH-9C granite discordantly intruding deformed Liv Group (Fairweather Formation) marbles and interbedded volcanic rocks as exemplified in Figure 11 (a,b). Sample GBH-9C is a titanite-bearing hornblende-biotite granite (Figure 6 and Appendix B). Hornblende from sample GBH-9C has a well-defined $^{40}Ar/^{39}Ar$ plateau age of 509 ± 3 Ma (2 sigma; 9 fractions, 92% ^{39}Ar release, MSWD = 0.5) (Figure 12). We consider this age to reflect cooling through the Ar retention temperature for this mineral (578°C to 490°C; Harrison 1982). Biotite from sample GBH-9C produced an irregular stepping up age spectrum during incremental heating (Figure 12). No isochron age determination was possible because of the generally homogenous radiogenic content of the step-heat releases. The biotite plateau age, 539 ± 6 Ma is not reasonable given the inverse age relations between the hornblende (younger, higher closure temperature) and biotite age (older, lower closure temperature), suggesting the biotite plateau age is not reflective of the geological cooling age for this mineral phase. Biotite is a known hydrous mineral that can be unstable during in vacuo laser heating (Gaber *et al*. 1988), and thus may not produce geologically meaningful gas release patterns that reflect crystal spatial Ar isotopic gradients (e.g. Brownlee and Renne 2010). Hence, we prefer the integrated age of 493 ± 5 Ma as most representative of the cooling age of this biotite mineral phase through Ar retention (345°C to 280°C; Harrison *et al*. 1985) from sample GBH-9C. The 509 ± 3 Ma (hornblende) and 493 ± 5 Ma (biotite) ages are younger than and therefore permissible of a 521 ± 7 Ma $^{206}Pb/^{238}$ U crystallization age for deformed metavolcanic rocks within the Fairweather Formation at the same sample locality (Paulsen *et al*. 2018), as well as the field relations that indicate the Fairweather Formation is older than the undeformed granite. The combination of these ages place deformation recorded by the Fairweather Formation to be within 528–506 Ma (Cambrian, Terreneuvian to Series 3) at this locality.

7. Discussion

All of the new U-Pb zircon ages obtained for orthogneisses and undeformed intrusive rocks of this study have yielded early Palaeozoic (515–486 Ma) crystallization ages, indicating emplacement concomitant with other ~535-480 Ma (Cambrian, Terreneuvian to Furongian) intrusive and volcanic (Liv Group) rocks associated with the Queen Maud batholith (Figure 3; Encarnación and Grunow 1996; Vogel *et al*. 2002; Paulsen *et al*. 2013, Paulsen *et al*. 2018). The results therefore indicate that the orthogneisses and undeformed intrusive rock samples of this study represent elements of the Queen Maud batholith. The new plutonic crystallization ages reported in this paper and Liv Group volcanic ages recently published in Paulsen *et al*. (2018) substantially add to our understanding of the timing of magmatism within this sector of the orogen, thereby warranting an examination of the patterns of magmatic activity with respect to time. Figure 13 shows a kernel density estimation diagram for all U-Pb zircon ages (n = 27) obtained for intrusive rocks, as well as extrusive (volcanic) samples (Liv Group) recently reported for the study area (Paulsen *et al*. 2013, 2018). The density analysis yields polymodal age distributions with 516 Ma, 506–502 Ma, and 488 Ma age peaks that are broadly similar to U-Pb detrital zircon age peaks shown by sandstones from the area. Cumulative analyses of igneous (n = 47) and detrital zircon U-Pb ages on the larger scale of the Queen Maud-Horlick Mountains yield similar results with 517 Ma, 506–503 Ma, and 486 Ma age peaks, a pattern that suggests that these time periods likely mark significant regional magmatic flare-ups within the larger Queen Maud batholith.

On a regional scale, the 517 Ma and 506–503 Ma magmatic flare-ups identified here are remarkably similar in age to other early and middle to late Cambrian intra-arc and back-arc successions found over this large region along the Pacific-Gondwana convergent margin from the Pensacola Mountains to southeast Australia (Rowell *et al*. 1997; Van Schmus *et al*. 1997; Duebendorfer and Rees 1998; Stump *et al*. 2004; Goodge *et al*. 2004a, 2012; Foster *et al*. 2005; Hagen-Peter *et al*. 2015; Hagen-Peter and Cottle 2016; Jago *et al*. 2019; Foden *et al*. 2020). The temporal correlation of Antarctic and Australian successions led Squire and Wilson (2005) to suggest that two synchronous short-lived magmatic flare-ups occurred along the Pacific-Gondwana convergent margin at c. 516–514 Ma and 504–500 Ma. They attributed magmatism associated

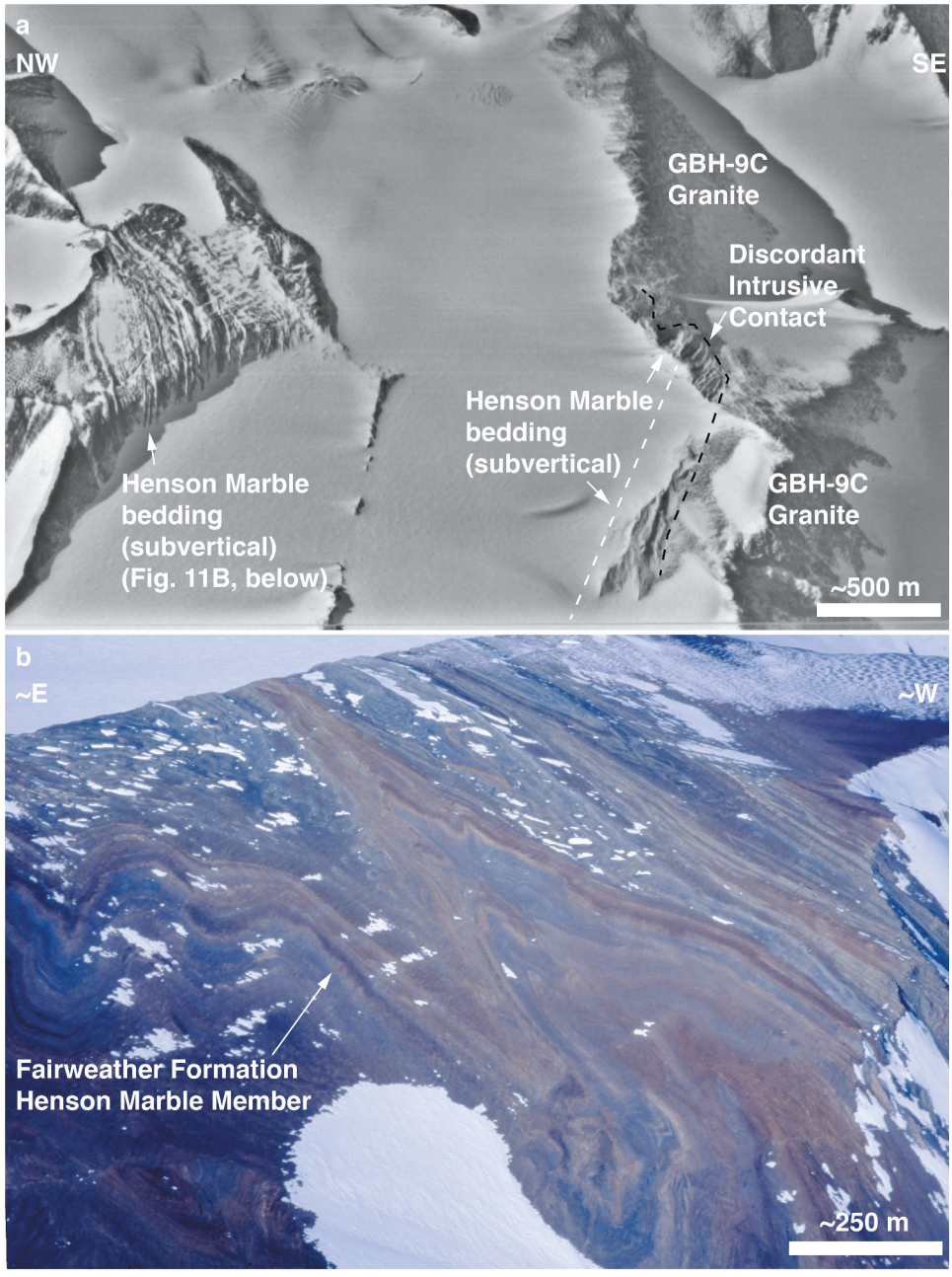

Figure 11. (a) Aerial photo (TMA1132) of the GBH-9C granite and its discordant intrusive contact with the steeply-dipping Henson Marble Member of the Fairweather Formation, and (b) Photo of the tightly-folded Henson Marble Member of the Fairweather Formation located ~5 km to the north of the GBH-9C sample locality (left part of Figure 11(a)).

with each pulse to upper plate extension induced by major slab rollback events that punctuated what were otherwise contractional phases of Ross-Delamerian orogenesis. The timing of these magmatic episodes shows remarkable coincidence with the 517 Ma and 506–503 Ma flare-ups in the Queen Maud batholith, although the U-Pb detrital zircon and igneous crystallization ages indicate that magmatism associated with each pulse spanned greater time intervals along with this sector of the Pacific-Gondwana margin, in particular, for those ages associated with the older 517 Ma age peak. The final 486 Ma peak correlates with emplacement of largely undeformed granitoid plutons and volcanic rocks during terminal Ross magmatism.

Figure 14 illustrates the temporal relation of deformation age constraints to the magmatic flare-ups provided by the new data presented here, along with existing data for the area of the Queen Maud batholith. Taken together, the age brackets provide important new evidence showing that deformation is constrained to primarily lie within the Cambrian (Series 2) to Ordovician (Lower) in the Queen Maud-Horlick Mountains sector of

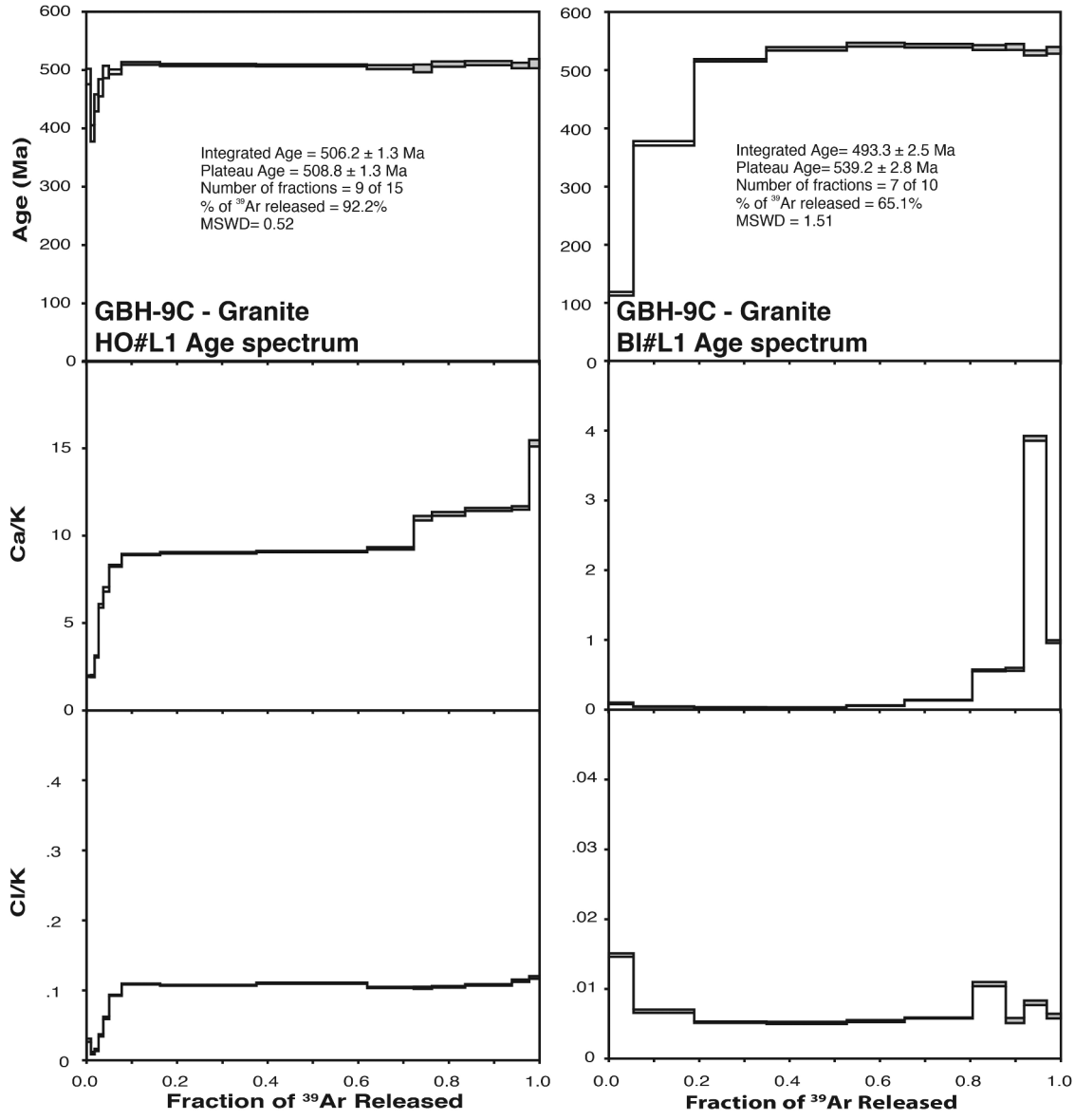

Figure 12. $^{40}Ar/^{39}Ar$ incremental release spectra for hornblende and biotite mineral separates from sample GBH-9C from the Polaris Peak area near Gough Glacier. Vertical axes represent age (Ma), and ratios of Ca/K and Cl/K calculated from released Ar isotopes; horizontal axis is cumulative percent ^{39}Ar released. Ages in the figure are reported at the ±1-sigma level, but are reported at the ±2-sigma level in the text. HO: hornblende, BI: biotite.

the Ross orogen, with some regions containing metamorphic and undeformed intrusive rocks indicating a transition to post-tectonic magmatism and cooling from ~508-470 Ma. In detail, deformation is locally documented to predate emplacement of igneous rocks associated with magmatic flare-ups in the Queen Maud batholith, for example, in the Scott Glacier area where hypabyssal intrusions of the 526 Ma Wyatt Formation intrude the folded La Gorce Formation (Stump 1986; Encarnación and Grunow 1996). Curtis *et al*. (2004) attributed this pattern to magmatism operating in concert with polycyclic changes between shortening and neutral or extensional strain regimes in the overriding Ross-Delamerian margin.

The ages associated with the older (517 Ma) and the younger (506–503 Ma and 486 Ma) plutonic magmatic flare-ups generally correlate with the older (Wyatt, Ackerman, Fairweather, and Leverett formations) and younger (Taylor and Greenlee formation) elements of the volcanic-sedimentary Cambrian Liv Group (Figure 3). Folds and disjunctive pressure solution cleavage in the Fairweather and Taylor formations indicate

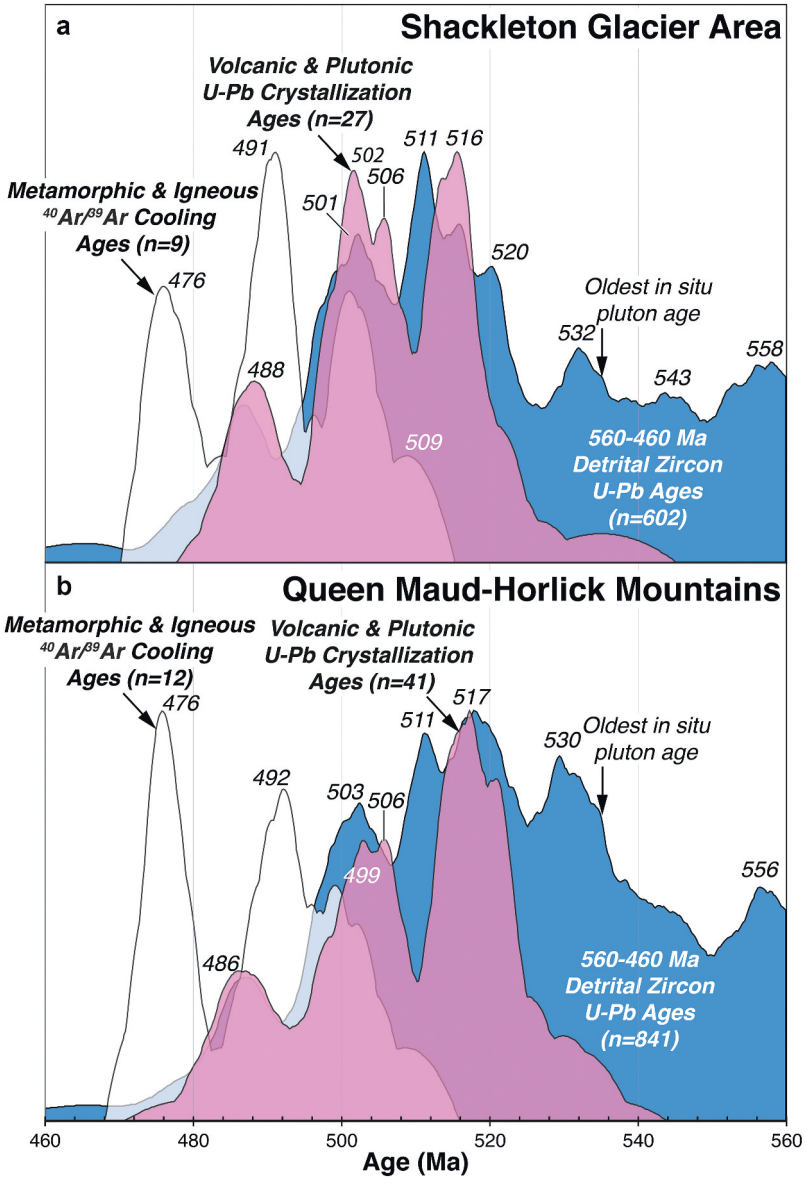

Figure 13. Stacked kernel density estimation diagrams (Vermeesch 2012) for U-Pb igneous crystallization ages and detrital zircon ages falling within the 560–460 Ma time period from the (A) Shackleton Glacier area (Ramsey to Liv glaciers); and (B) the broader Queen Maud-Horlick Mountains sectors of the Ross orogen of which the Shackleton Glacier area is part. Detrital zircon ages are compiled for the Liv and Beardmore groups from Stump *et al*. (2007) and Paulsen *et al*. (2015), (2017)). Volcanic and plutonic U-Pb crystallization ages are compiled from data presented in this paper, as well as Encarnación and Grunow (1996), Van Schmus *et al*. (1997), Encarnación *et al*. (1999), Vogel *et al*. (2002), and Paulsen *et al*. (2013, 2016c, 2018). $^{40}Ar/^{39}Ar$ cooling ages are compiled from data presented in this paper, as well as (Paulsen *et al*. 2004, 2008, 2013).

that contraction must post-date their early to middle Cambrian depositional ages (Stump 1981, 1986; Van Schmus *et al*. 1997; Encarnación *et al*. 1999; Paulsen *et al*. 2015, 2018). The 509 ± 3 Ma $^{40}Ar/^{39}Ar$ hornblende cooling age from the undeformed granite (GBH-9C) at Polaris Peak assumes regional significance because it provides the earliest minimum age for the deformation of an older stratigraphic package bracketed between 528 Ma and 506 Ma (Cambrian, Terreneuvian to Series 3) in the Shackleton Glacier area. Deformation at this site may have occurred between the 517 and 506–503 Ma magmatic flare-ups identified here. However, the relatively large time spans that are bracketed by the younger and older age limits for deformation and lack of exposed or recognized angular unconformities hamper a more definitive evaluation of this hypothesis.

Figure 15 illustrates the spatial and temporal relation of deformation within the Queen Maud-Horlick Mountains to other areas in the central Transantarctic

Mountains and south Victoria land. The diagram does not depict all isotopic ages determined for rocks from these provinces, but selectively shows those ages that provide the best age constraints for deformation timing. Younger age limits on deformation timing are typically provided by crystallization ages of undeformed igneous rocks, but also include cooling ages of igneous and metamorphic rocks. In some cases, the only younger limits on the age of deformation are the Devonian through Triassic Beacon Supergroup, which unconformably overlies metasedimentary and plutonic rocks of the Ross orogenic belt. In most areas, the older limits on deformation are provided by the youngest dated detrital minerals (zircons or mica) or igneous rocks that are deformed. Of course, the older age limit on deformation does not preclude earlier deformational phases. For example, this is the case for localities in south Victoria Land and the Miller Range where we have used older ages for igneous rocks that have been interpreted to have been emplaced concomitant with contraction in the overriding plate. In a similar sense, the youngest age limit on deformation does not preclude later deformation phases, which is possible if strains were localized or insufficient to induce foliations in igneous rocks due to

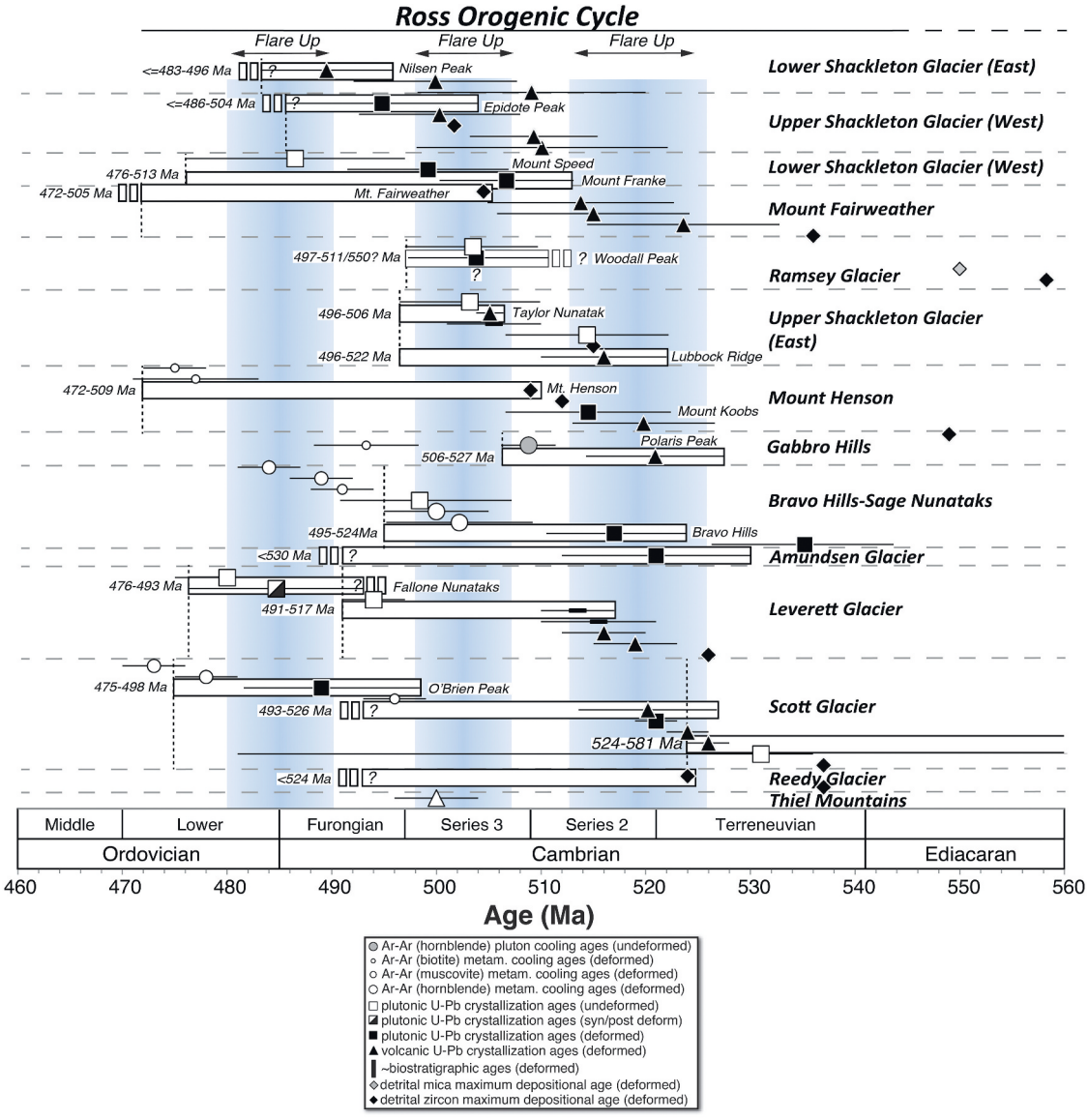

Figure 14. Diagram summarizing the available age constraints for magmatism, deformation, and metamorphic cooling within the Ross orogen in the Queen Maud and Horlick mountains. Errors on ages are shown by horizontal black lines. White bar indicates upper and lower age constraints (range identified) for deformation at the localities. Ages are from this study and compiled from Encarnación and Grunow (1996), Rowell *et al*. (1997), Van Schmus *et al*. (1997), Encarnación *et al*. (1999), Grunow and Encarnación (2000b), Stump *et al*. (2007), and Paulsen *et al*. (2004, 2008, 2013, 2015, 2016c, 2017, 2018).

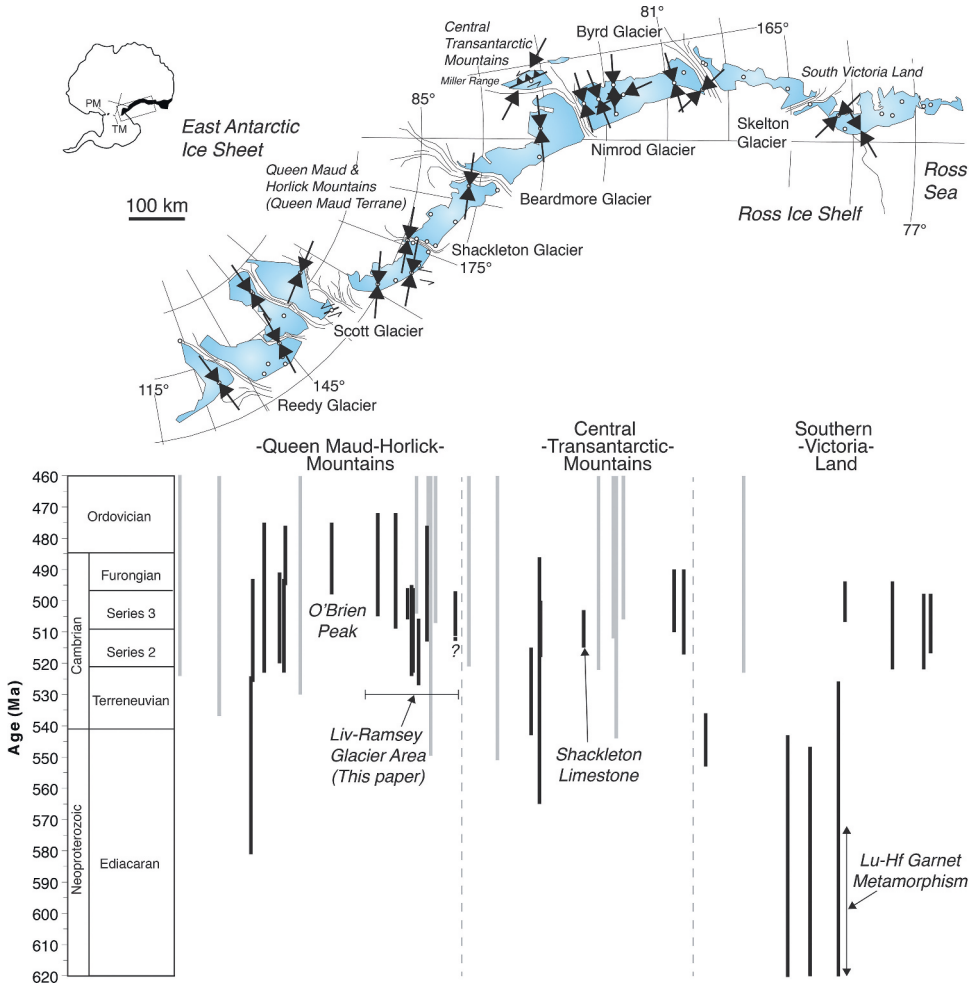

Figure 15. Diagram summarizing the available age constraints and general contraction directions for deformation within the Ross orogen in the Queen Maud and Horlick mountains with respect to ages and deformation from the central Transantarctic Mountains and southern Victoria Land. Grey bars indicate age ranges that lack younger age constraints within the timescale shown. Double inward pointing arrows on the map show shortening directions that are primarily drawn at a high angle to the strike direction of metasedimentary rocks in the range, assuming contraction is at a high angle to strike of tilted beds and cleavage (where reported) from Grindley and McDougall (1969), McGregor and Wade (1969), Mirsky (1969), Warren (1969), Stump (1986), and Paulsen *et al*. (2004); arrows in Miller Range indicate top-to-the-southeast shear (with a left-lateral component) reported by Goodge *et al*. (1993a). Localities with evidence of translational movement (with shear sense reported) in the O'Brien Peak and Shackleton Glacier areas are from Paulsen *et al*. (2004, 2008). Overall the contraction directions vary from range-normal to rotated clockwise relative to the range. Such a pattern, combined with the translational shear zones that are present, is consistent with a sinistral oblique subduction direction (Goodge *et al*. 1993a), as well as changes in the trends of structural belts wrapping around the promontories and embayments of marginal basins and blocks along the East Antarctic cratonic margin (Paulsen *et al*. 2004). Inset map shows geographical extent of the sector of the Ross orogen in Antarctica depicted in figure. Small white circles show approximate locations of sample sites from which age constraints have been derived. Abbreviations: PM, Pensacola Mountains; TM, Thiel Mountains. Ages compiled from Cook and Craw (2001), Cottle and Cooper (2006), Encarnación and Grunow (1996), Van Schmus *et al*. (1997), Encarnación *et al*. (1999), Goodge *et al*. (2012), Goodge *et al*. (1993b, 2004a, 2004b), Grunow and Encarnación (2000a), Hagen-Peter and Cottle (2016), Hagen-Peter *et al*. (2015), Hagen-Peter and Cottle (2016), Hall *et al*. (1995), Myrow *et al*. (2002), Paulsen *et al*. (2004, 2007, 2008, 2013, 2015, 2017, 2018), Stump *et al*. (2004, 2007), and Talarico *et al*. (2007)

their differing material properties. These same caveats apply to the temporal constraints on deformation in the Shackleton Glacier area shown in Figure 14. Indeed, the youngest deformation in the Shackleton Glacier area is constrained to ≤496 Ma at Nilsen Peak, where mylonitic shearing of the Taylor Formation appears to post-date ≥506 Ma shortening of the Fairweather Formation at Polaris Peak, yet deformation at both localities presumably relate to the overall suite of processes operating in association with the Ross orogenic cycle.

The oldest deformation yet documented is in south Victoria Land, where Skelton Group sandstones, pelites, and marbles were deformed and metamorphosed during an early phase of presumed shortening at

c. 590–570 Ma and perhaps as early as c. 615–610 Ma (Figure 15) (Hagen-Peter *et al*. 2016). The deformation identified elsewhere in exposed sectors of the Ross orogen is younger and may ultimately be related to plate motion changes commencing at ~515-510 Ma (Grunow *et al*. 1996; Boger and Miller 2004; Squire and Wilson 2005; Squire *et al*. 2006). This possibility is supported by roughly synchronous deformation found elsewhere along the Pacific-Gondwana margin. In the Pensacola Mountains, syn-deformational intrusive rocks have 505 ±5 Ma U-Pb crystallization ages (Figure 2) (Curtis *et al*. 2004). In the Delamerian orogen of south Australia, back-arc extension was interrupted by two to three periods of contraction in the middle to late Cambrian (Foden *et al*. 2020). In Tasmania, ophiolite obduction occurred at 515–510 Ma, whereas $^{40}Ar/^{39}Ar$ ages record rapid cooling at 508 Ma interpreted to reflect post-orogenic extension during subsequent slab steepening or rollback (Foster *et al*. 2005). Associated with this extensional phase was the eruption of the 505–495 Ma Mount Read-Mount Stavely back-arc volcanic complexes in Tasmania and southeast Australia (Foster *et al*. 2005), which correlate in age with late middle Cambrian volcanic-sedimentary successions in the Bowers back-arc basin in north Victoria Land (Jago *et al*. 2019), the Ellsworth-Whitmore Mountains (Duebendorfer and Rees 1998), the Pensacola Mountains (Millar and Storey 1995; Van Schmus *et al*. 1997; Rowell *et al*. 2001), and the 506–503 Ma magmatic pulse documented here for the Queen Maud batholith. Subsequent late Cambrian to early Ordovician contractional deformation impacted many of these areas (Crawford and Berry 1992; Storey *et al*. 1996; Duebendorfer and Rees 1998; Foster *et al*. 2005; Rossetti *et al*. 2011; Estrada *et al*. 2016; Paulsen *et al*. 2016a; Jago *et al*. 2019; Foden *et al*. 2020).

8. Conclusion

The data presented in this paper provide important new evidence that further demonstrates a notable correlation of magmatic and deformational timing along the Pacific-Gondwana margin. The magmatic and deformational age constraints are consistent with the concept that rocks of the Queen Maud-Horlick Mountains share a similar petrotectonic history with other localities along the Pacific-Gondwana margin (Rowell *et al*. 1992). The results suggest that rocks in the Shackleton Glacier region of the Queen Maud-Horlick Mountains are not part of Precambrian cratonic crust and are not particularly exotic with respect to other petrotectonic provinces found along the paleo-Pacific margin of Gondwana, but instead developed within, and reflect tectonomagmatic processes along, the dominantly subduction-related peri-Gondwana realm. The similar timing of events over such a large area of the Pacific-Gondwana margin suggests that tectonism may have occurred in response to plate reorganization associated with the terminal assembly of Gondwana.

Acknowledgments

Several samples analyzed for this work came from the Polar Rock Repository, Byrd Polar and Climate Research Center, the Ohio State University, doi:10.7289/V5RF5S18. The Arizona LaserChron Center is supported by National Science Foundation Grant EAR-0443387. Fieldwork was supported by the Office of Polar Programs, U.S. National Science Foundation.

Disclosure statement

No potential conflict of interest was reported by the authors.

Funding

This work was supported by the LaserChron Center [NSF EAR-0443387]; Tim Paulsen [NSF OPP-0835480, University of Wisconsin Oshkosh]; John Encarnación [NSF OPP-]; Anne Grunow [NSF OPP-9317673].

References

Benowitz, J.A., Layer, P.W., and Vanlaningham, S., 2014, Persistent long-term (c. 24 Ma) exhumation in the Eastern Alaska Range constrained by stacked thermochronology, *in* Jourdan, F., Mark, D.F., and Verati, C., eds., Advances in $^{40}Ar/^{39}Ar$ dating: From archaeology to planetary sciences: Geological Society of London, Special Publication, London, v. 378, p. 225–243.

Black, L.P., Kamo, S.L., Allen, C.M., Davis, D.W., Aleinikoff, J.N., Valley, J.W., Mundil, R., Campbell, I.H., Korsch, R.J., Williams, I. S., and Foudoulis, C., 2004, Improved Pb-206/U-238 microprobe geochronology by the monitoring of a trace-element-related matrix effect; SHRIMP, ID-TIMS, ELA-ICP-MS and oxygen isotope documentation for a series of zircon standards: Chemical Geology, v. 205, p. 115–140.

Boger, S.D., 2011, Antarctica — Before and after Gondwana: Gondwana Research, v. 19, p. 335–371, doi:10.1016/j.gr.2010.09.003

Boger, S.D., and Miller, J.M., 2004, Terminal suturing of Gondwana and the onset of the Ross-Delamerian Orogeny: The cause and effect of an Early Cambrian reconfiguration of plate motions: Earth and Planetary Science Letters, v. 219, p. 35–48, doi:10.1016/S0012-821X(03)00692-7

Borg, S.G., and DePaolo, D.J., 1991, A tectonic model of the Antarctic Gondwana margin with implications for southeastern Australia: Isotopic and geochemical evidence: Tectonophysics, v. 196, p. 339–358, doi:10.1016/0040-1951(91)90329-Q

Borg, S.G., and DePaolo, D.J., 1994, Laurentia, Australia, and Antarctica as a Late Proterozoic supercontinent: Constraints from isotopic mapping: Geology, v. 22, p. 307–310, doi:10.1130/0091-7613(1994)022<0307:LAAAAA>2.3.CO;2

Borg, S.G., DePaolo, D.J., and Smith, B.M., 1990, Isotopic structure and tectonics of the central Transantarctic mountains: Journal of Geophysical Research Solid Earth, v. 95, p. 6647–6667, doi:10.1029/JB095iB05p06647

Brownlee, S.J., and Renne, P.R., 2010, Thermal history of the Ecstall pluton from $^{40}Ar/^{39}Ar$ geochronology and thermal modeling: Geochimica et Cosmochimica Acta, v. 74, p. 4375–4391, doi:10.1016/j.gca.2010.04.023

Burgener, J.D., 1975, Petrography of the Queen Maud batholith, central Transantarctic Mountains, Ross Dependency, Antarctica [M.S. thesis]: Madison, University of Wisconsin, 32 p.

Cawood, P.A., 2005, Terra Australis Orogen: Rodinia breakup and development of the Pacific and Iapetus margins of Gondwana during the Neoproterozoic and Paleozoic: Earth-Science Reviews, v. 69, p. 249–279, doi:10.1016/j.earscirev.2004.09.001

Cohen, K.M., Finney, S.C., Gibbard, P.L., and Fan, J.-X., 2013, The ICS International Chronostratigraphic Chart: Episodes, v. 36, p. 199–204, doi:10.1111/j.1502-3931.1980.tb01026.x

Cook, Y.A., and Craw, D., 2001, Amalgamation of disparate crustal fragments in the Walcott Bay-Foster Glacier area, South Victoria Land, Antarctica: New Zealand Journal of Geology and Geophysics, v. 44, p. 403–416, doi:10.1080/00288306.2001.9514947

Cottle, J.M., and Cooper, A.F., 2006, Geology, geochemistry, and geochronology of an A-type granite in the Mulock Glacier area, southern Victoria Land, Antarctica: New Zealand Journal of Geology and Geophysics, v. 49, p. 191–202, doi:10.1080/00288306.2006.9515159

Crawford, A.J., and Berry, R.F., 1992, Tectonic implications of Late Proterozoic-Early Palaeozoic igneous rock associations in western Tasmania: Tectonophysics, v. 214, p. 37–56, doi:10.1016/0040-1951(92)90189-D

Curtis, M.L., Millar, I.L., Storey, B.C., and Fanning, M., 2004, Structural and geochronological constraints of early Ross orogenic deformation in the Pensacola Mountains, Antarctica: Geological Society of America Bulletin, v. 116, p. 619–636, doi:10.1130/B25170.1

Davis, M.B., and Blankenship, D.D., 2005, Geology of the Scott-Reedy glaciers area southern Transantarctic Mountains, Antarctica: Geological Society of America Map Chart Series MCH093, scale 1:500,000, 1 sheet, doi:10.1130/2005.MCH093.

Duebendorfer, E.M., and Rees, M.N., 1998, Evidence for Cambrian deformation in the Ellsworth-Whitmore Mountains terrane, Antarctica: Stratigraphic and tectonic implications: Geology, v. 26, p. 55–58, doi:10.1130/0091-7613(1998)026<0055:EFCDIT>2.3.CO;2

Encarnación, J., and Grunow, A., 1996, Changing magmatic and tectonic styles along the paleo-Pacific margin of Gondwana and the onset of early Paleozoic magmatism in Antarctica: Tectonics, v. 15, p. 1325–1341, doi:10.1029/96TC01484

Encarnación, J., Rowell, A.J., and Grunow, A.M., 1999, A U-Pb Age for the Cambrian Taylor Formation, Antarctica: Implications for the Cambrian Time Scale: The Journal of Geology, v. 107, p. 497–504, doi:10.1086/314361

Estrada, S., Läufer, A., Eckelmann, K., Hofmann, M., Gärtner, A., and Linnemann, U., 2016, Continuous Neoproterozoic to Ordovician sedimentation at the East Gondwana margin — Implications from detrital zircons of the Ross Orogen in northern Victoria Land, Antarctica: Gondwana Research, v. 37, p. 426–448, doi:10.1016/j.gr.2015.10.006

Faure, G., Eastin, R., Ray, P.T., Mclelland, D., and Shultz, C.H., 1979, Geochronology of igneous and metamorphic rocks, central Transantarctic Mountains, *in* 4th International Gondwana Symposium: papers, Calcutta, India, Hindustan Publishing Corporation, p. 805–813.

Felder, R.P., and Faure, G., 1979, Investigation of an anomalous date for Lonely Ridge granodiorite, Nilsen Plateau, Transantarctic Mountains: Antarctic Journal of the United States, v. 14, p. 24.

Foden, J., Elburg, M., Turner, S., Clark, C., Blades, M.L., Cox, G., Collins, A.S., Wolff, K., and George, C., 2020, Cambro-Ordovician magmatism in the Delamerian orogeny: Implications for tectonic development of the southern Gondwanan margin: Gondwana Research, v. 81, p. 490–521, doi:10.1016/j.gr.2019.12.006

Foster, D.A., Gray, D.R., and Spaggiari, C., 2005, Timing of subduction and exhumation along the Cambrian East Gondwana margin, and the formation of Paleozoic backarc basins: Geological Society of America Bulletin, v. 117, p. 105–116, doi:10.1130/B25481.1

Gaber, I.J., Foland, K.A., and Corbato, C.E., 1988, On the significance of argon release from biotite and amphibole during $^{40}Ar/^{39}Ar$ vacuum heating: Geochimica et Cosmochimica Acta, v. 52, p. 2457–2465, doi:10.1016/0016-7037(88)90304-3

Gehrels, G.E., Valencia, V.A., and Ruiz, J., 2008, Enhanced precision, accuracy, efficiency, and spatial resolution of U-Pb ages by laser ablation-multicollector-inductively coupled plasma-mass spectrometry: Geochemistry, Geophysics, Geosystems, v. 9, p. 1–13, doi:10.1029/2007GC001805

González, P.D., Sato, A.M., Naipauer, M., Varela, R., Basei, M., Sato, K., Llambías, E.J., Chemale, F., and Dorado, A.C., 2018, Patagonia-Antarctica Early Paleozoic conjugate margins: Cambrian synsedimentary silicic magmatism, U-Pb dating of K-bentonites, and related volcanogenic rocks: Gondwana Research, v. 63, p. 186–225, doi:10.1016/j.gr.2018.05.015

Goodge, J.W., 1997, Latest Neoproterozoic basin inversion of the Beardmore Group, central Transantarctic Mountains, Antarctica: Tectonics, v. 16, p. 682–701, doi:10.1029/97TC01417

Goodge, J.W., 2020, Geological and tectonic evolution of the Transantarctic Mountains, from ancient craton to recent enigma: Gondwana Research, v. 80, p. 50–122, doi:10.1016/j.gr.2019.11.001

Goodge, J.W., Fanning, C.M., Norman, M.D., and Bennett, V.C., 2012, Temporal, isotopic and spatial relations of early Paleozoic Gondwana-margin arc magmatism, Central Transantarctic Mountains, Antarctica: Journal of Petrology, v. 53, p. 2027–2065, doi:10.1093/petrology/egs043

Goodge, J.W., Hansen, V.L., Peacock, S.M., Smith, B.K., and Walker, N.W., 1993a, Kinematic evolution of the Miller Range Shear Zone, Central Transantarctic Mountains, Antarctica, and implications for Neoproterozoic to Early Paleozoic tectonics of the East Antarctic Margin of Gondwana: Tectonics, v. 12, p. 1460–1478, doi:10.1029/93TC02192

Goodge, J.W., Myrow, P., Phillips, D., Fanning, C.M., and Williams, I.S., 2004a, Siliciclastic record of rapid denudation in response to convergent-margin orogenesis, Ross Orogen, Antarctica, *in* Bernet, M., and Spiegel, C., eds., Detrital thermochronology – Provenance analysis, exhumation, and landscape evolution of mountain belts: Geological Society of America, Special Paper, v. 378, p. 105-126, Boulder, Colorado, oldoi:10.1130/0-8137-2378-7.105

Goodge, J.W., Myrow, P., Williams, I.S., and Bowring, S.A., 2002, Age and Provenance of the Beardmore Group, Antarctica: Constraints on Rodinia Supercontinent Breakup: Journal of Geology, v. 110, p. 393–406, doi:10.1086/340629

Goodge, J.W., Walker, N.W., and Hansen, V.L., 1993b, Neoproterozoic-Cambrian basement-involved orogenesis within the Antarctic margin of Gondwana: Geology, v. 21, p. 37–40, doi:10.1130/0091-7613(1993)021<0037:NCBIOW>2.3.CO;2

Goodge, J.W., Williams, I.S., and Myrow, P., 2004b, Provenance of Neoproterozoic and lower Paleozoic siliciclastic rocks of the central Ross orogen, Antarctica: Detrital record of rift-, passive-, and active-margin sedimentation: Geological Society of America Bulletin, v. 116, 9, p. 1253–1279, doi:10.1130/B25347.1

Grindley, G.W., and McDougall, I., 1969, Age and correlation of the Nimrod Group and other precambrian rock units in the central Transantarctic Mountains, Antarctica: New Zealand Journal of Geology and Geophysics, v. 12, p. 391–411, doi:10.1080/00288306.1969.10420290

Grunow, A.M., and Encarnación, J., 2000a, Terranes or Cambrian polar wander: New data from the Scott Glacier area: Transantarctic Mountains, Antarctica: Tectonics, v. 19, p. 168–181.

Grunow, A.M., and Encarnación, J.P., 2000b, Cambro-Ordovician palaeomagnetic and geochronologic data from southern Victoria Land, Antarctica: Revision of the Gondwana apparent polar wander path: Geophysical Journal International, v. 141, p. 392–400, doi:10.1046/j.1365-246x.2000.00083.x

Grunow, A.M., Hanson, R., and Wilson, T., 1996, Were aspects of Pan-African deformation linked to Iapetus opening?: Geology, v. 24, p. 1063–1066, doi:10.1130/0091-7613(1996)024<1063:WAOPAD>2.3.CO;2

Hagen-Peter, G., and Cottle, J.M., 2016, Synchronous alkaline and subalkaline magmatism during the late Neoproterozoic – Early Paleozoic Ross orogeny, Antarctica: Insights into magmatic sources and processes within a continental arc: Lithos, v. 262, p. 677–698, doi:10.1016/j.lithos.2016.07.032

Hagen-Peter, G., Cottle, J.M., Smit, M., and Cooper, A.F., 2016, Coupled garnet Lu-Hf and monazite U-Pb geochronology constrain early convergent margin dynamics in the Ross orogen, Antarctica: Journal of Metamorphic Geology, v. 34, p. 293–319, doi:10.1111/jmg.12182

Hagen-Peter, G., Cottle, J.M., Tulloch, A.J., and Cox, S.C., 2015, Mixing between enriched lithospheric mantle and crustal components in a short-lived subduction-related magma system, Dry Valleys area, Antarctica: Insights from U-Pb geochronology, Hf isotopes, and whole-rock geochemistry: Lithosphere, v. 7, p. 174–188, doi:10.1130/L384.1

Hall, C.E., Cooper, A.F., and Parkinson, D.L., 1995, Early Cambrian carbonatite in Antarctica: Journal of the Geological Society of London, v. 152, p. 721–728, doi:10.1144/gsjgs.152.4.0721

Harrison, T.M., 1982, Diffusion of ^{40}Ar in hornblende: Contributions to Mineralogy and Petrology, v. 78, p. 324–331, doi:10.1007/BF00398927

Harrison, T.M., Duncan, I., and Mcdougall, I., 1985, Diffusion of ^{40}Ar in biotite: Temperature, pressure and compositional effects: Geochimica et Cosmochimica Acta, v. 49, p. 2461–2468, doi:10.1016/0016-7037(85)90246-7

Hoskin, P.W.O., and Schaltegger, U., 2003, The composition of zircon and igneous and metamorphic petrogenesis: Reviews of Mineralogy and Geochemistry, v. 53, p. 27–62, doi:10.2113/0530027

Jago, J.B., Bentley, C.J., and Cooper, R.A., 2019, Cambrian biostratigraphy of the Bowers back-arc basin, Northern Victoria Land, Antarctica – A review: Palaeoworld, v. 28, p. 276–288, doi:10.1016/j.palwor.2018.12.002

Laird, M.G., 1981, Lower Palaeozoic rocks of Antarctica, *in* Holland, C.H., ed., Lower Palaeozoic of the Palaeozoic of the Middle East, Eastern Africa, and Antarctica: Chichester, New York, Brisbane, and Toronto; John Wiley, p. 257–314.

Laird, M.G., 1991, The late Proterozoic-middle Palaeozoic rocks of Antarctica, *in* Tingey, R.J., ed., The Geology of Antarctica: Oxford; Clarendon Press, p. 74–119.

Laird, M.G., Mansergh, G.D., and Chappell, J.M.A., 1971, Geology of the central Nimrod Glacier area, Antarctica: New Zealand Journal of Geology and Geophysics, v. 14, p. 427–468, doi:10.1080/00288306.1971.10421939

Layer, P.W., 2000, Argon-40/argon-39 age of the El'gygytgyn impact event, Chukotka, Russia: Meteoritics & Planetary Science, v. 35, p. 591–599, doi:10.1111/j.1945-5100.2000.tb01439.x

Layer, P.W., Hall, C.M., and York, D., 1997, The derivation of ^{40}Ar/^{39}Ar age spectra of single grains of hornblende and biotite by laser step heating: Geophysical Research Letters, v. 14, p. 757–760, doi:10.1029/GL014i007p00757

Ludwig, K., 2008, Isoplot 3.6: Berkeley Geochronology Center. Special Publication, Berkeley, California, v. 4, 77 p.

McDougall, I., and Harrison, T.M., 1991, Geochronology and thermochronology by the ^{40}Ar/^{39}Ar method-2nd edition: New York, Oxford University Press, 288 p.

McGregor, V.R., 1965, Notes on the geology of the area between the heads of the Beardmore and Shackleton glaciers, Antarctica: New Zealand Journal of Geology and Geophysics, v. 8, p. 278–291, doi:10.1080/00288306.1965.10428111

McGregor, V.R., and Wade, F.A., 1969, Geology of the western Queen Maud Mountains: American Geographical Society Antarctic Map Folio Series (folio 12, plate 15), scale: 1:1,000,000.

McKenzie, N.R., Hughes, N.C., Gill, B.C., and Myrow, P.M., 2014, Plate tectonic influences on Neoproterozoic-early Paleozoic climate and animal evolution: Geology, v. 42, p. 127–130, doi:10.1130/G34962.1

Millar, I.L., and Storey, B.C., 1995, Early Palaeozoic rather than Neoproterozoic volcanism and rifting within the Transantarctic Mountains: Journal of the Geological Society of London, v. 152, p. 417–420, doi:10.1144/gsjgs.152.3.0417

Mirsky, A., 1969, Geology of the Ohio Range–Liv Glacier area: American Geographical Society Antarctic Map Folio Series (folio 12, plate 16), scale: 1:1,000,000.

Murtaugh, J.G., 1969, Geology of the Wisconsin Range batholith, Transantarctic Mountains: New Zealand Journal of

Geology and Geophysics, v. 12, p. 526–550, doi:10.1080/00288306.1969.10420297

Myrow, P.M., Pope, M.C., Goodge, J.W., Fischer, W., and Palmer, A.R., 2002, Depositional history of pre-Devonian strata and timing of Ross orogenic tectonism in the central Transantarctic Mountains, Antarctica: Geological Society of America Bulletin, v. 114, p. 1070–1088, doi:10.1130/0016-7606(2002)114<1070:DHOPDS>2.0.CO;2

Paulsen, T.S., Deering, C., Sliwinski, J., Bachmann, O., and Guillong, M., 2016a, Detrital zircon ages from the Ross Supergroup, north Victoria Land, Antarctica: Implications for the tectonostratigraphic evolution of the Pacific-Gondwana margin: Gondwana Research, v. 35, p. 79–96, doi:10.1016/j.gr.2016.04.001

Paulsen, T.S., Deering, C., Sliwinski, J., Bachmann, O., and Guillong, M., 2016b, A continental arc tempo discovered in the Pacific-Gondwana margin mudpile?: Geology, v. 44, p. 915–918, doi:10.1130/G38189.1

Paulsen, T.S., Deering, C., Sliwinski, J., Bachmann, O., and Guillong, M., 2017, Evidence for a spike in mantle carbon outgassing during the Ediacaran period: Nature Geoscience, v. 10, p. 930–933, doi:10.1038/s41561-017-0011-6

Paulsen, T.S., Encarnación, J., Grunow, A., and Pecha, M., 2016c, Zircon U–Pb age constraints for a Cambrian age for metasedimentary rocks at O'Brien Peak, Antarctica: New Zealand Journal of Geology and Geophysics, v. 59, p. 592–597, doi:10.1080/00288306.2016.1182033

Paulsen, T.S., Encarnación, J., Grunow, A., Valencia, V.A., and Rasoazanamparany, C., 2008, Late sinistral shearing along Gondwana's paleo-Pacific margin in the Ross orogen, Antarctica: New structure and age data from the O'Brien Peak area: The Journal of Geology, v. 116, p. 303–312, doi:10.1086/587727

Paulsen, T.S., Encarnación, J., and Grunow, A.M., 2004, Structure and timing of transpressional deformation in the Shackleton Glacier area, Ross orogen, Antarctica: Journal of the Geological Society of London, v. 161, p. 1027–1038, doi:10.1144/0016-764903-040

Paulsen, T.S., Encarnación, J., Grunow, A.M., Layer, P.W., and Watkeys, M., 2007, New age constraints for a short pulse in Ross orogen deformation triggered by East-West Gondwana suturing: Gondwana Research, v. 12, p. 417–427, doi:10.1016/j.gr.2007.05.011

Paulsen, T.S., Encarnación, J., Grunow, A.M., Stump, E., Pecha, M., and Valencia, V.A., 2018, Correlation and late-stage deformation of Liv Group volcanics in the Ross-Delamerian orogen, Antarctica, from new U-Pb ages: The Journal of Geology, v. 126, p. 307–323, doi:10.1086/697036

Paulsen, T.S., Encarnación, J., Grunow, A.M., Valencia, V.A., Layer, P.W., Pecha, M., Stump, E., Roeske, S., Thao, S., and Rasoazanamparany, C., 2015, Detrital mineral ages from the Ross Supergroup, Antarctica: Implications for the Queen Maud terrane and outboard sediment provenance on the Gondwana margin: Gondwana Research, v. 27, p. 377–391, doi:10.1016/j.gr.2013.10.006

Paulsen, T.S., Encarnación, J., Grunow, A.M., Valencia, V.A., Pecha, M., Layer, P.W., and Rasoazanamparany, C., 2013, Age and significance of "outboard" high-grade metamorphics and intrusives of the Ross orogen, Antarctica: Gondwana Research, v. 24, p. 349–358, doi:10.1016/j.gr.2012.10.004

Renne, P.R., 1994, Intercalibration of astronomical and radioisotopic time: Geology, v. 22, p. 783–786, doi:10.1130/0091-7613(1994)022<0783:IOAART>2.3.CO;2

Renne, P.R., Mundil, R., Balco, G., Min, K., and Ludwig, K.R., 2010, Joint determination of ^{40}K decay constants and ^{40}Ar/^{40}K for the Fish Canyon sanidine standard, and improved accuracy for ^{40}Ar/^{39}Ar geochronology: Geochimica et Cosmochimica Acta, v. 74, p. 5349–5367, doi:10.1016/j.gca.2010.06.017

Rossetti, F., Vignaroli, G., Di Vincenzo, G., Gerdes, A., Ghezzo, C., Theye, T., and Balsamo, F., 2011, Long-lived orogenic construction along the paleo-Pacific margin of Gondwana (Deep Freeze Range, North Victoria Land, Antarctica): Tectonics, v. 30, doi:10.1029/2010TC002804

Rowell, A.J., Gonzales, D.A., McKenna, L.W., Evans, K.R., Stump, E., and Van Schmus, W.R., 1997, Lower Paleozoic rocks in the Queen Maud Mountains: Revised ages and significance, *in* Ricci, C.A., ed., The Antarctic Region: Geological Evolution and Processes: Siena, Italy; Terra Antarctica Publication, p. 201–207.

Rowell, A.J., and Rees, M.N., 1989, Early Palaeozoic history of the upper Beardmore Glacier area: Implications for a major Antarctic structural boundary within the Transantarctic Mountains: Antarctic Science, v. 1, p. 249–260, doi:10.1017/S0954102089000374

Rowell, A.J., Rees, M.N., and Evans, K.R., 1992, Evidence of major Middle Cambrian deformation in the Ross Orogen, Antarctica: Geology, v. 20, p. 31–34, doi:10.1130/0091-7613-(1992)020<0031:EOMMCD>2.3.CO;2

Rowell, A.J., van Schmus, W.R., Storey, B.C., Fetter, A.H., and Evans, K.R., 2001, Latest Neoproterozoic to mid-Cambrian age for the main deformation phases of the Transantarctic Mountains: New stratigraphic and isotopic constraints from the Pensacola Mountains, Antarctica: Journal of the Geological Society of London, v. 158, p. 295–308, doi:10.1144/jgs.158.2.295

Rubatto, D., 2002, Zircon trace element geochemistry: Partitioning with garnet and the link between U-Pb ages and metamorphism: Chemical Geology, v. 184, p. 123–138, doi:10.1016/S0009-2541(01)00355-2

Samson, S.D., and Alexander, E.C., 1987, Calibration of the interlaboratory ^{40}Ar/^{39}Ar dating standard, MMhb1: Chemical Geology, v. 66, p. 27–34.

Squire, R.J., Campbell, I.H., Allen, C.M., and Wilson, C.J.L., 2006, Did the Transgondwanan Supermountain trigger the explosive radiation of animals on Earth?: Earth and Planetary Science Letters, v. 250, p. 116–133, doi:10.1016/j.epsl.2006.07.032

Squire, R.J., and Wilson, C.J.L., 2005, Interaction between collisional orogenesis and convergent-margin processes: Evolution of the Cambrian proto-Pacific margin of East Gondwana: Journal of the Geological Society of London, v. 162, p. 749–761, doi:10.1144/0016-764904-087

Stacey, J.S., and Kramers, J.D., 1975, Approximation of terrestrial lead isotope evolution by a two-stage model: Earth and Planetary Science Letters, v. 26, p. 207–221, doi:10.1016/0012-821X(75)90088-6

Storey, B.C., Macdonald, D.I.M., Dalziel, I.W.D., Isbell, J.L., and Millar, I.L., 1996, Early Paleozoic sedimentation, magmatism, and deformation in the Pensacola Mountains, Antarctica: The significance of the Ross orogeny: Geological Society of America Bulletin, v. 108, p. 685–707, doi:10.1130/0016-7606-(1996)108<0685:EPSMAD>2.3.CO;2

Streckeisen, A., 1974, Classification and nomenclature of plutonic rocks: Recommendations of the IUGS subcommission on the systematics of igneous rocks: Geologische Rundschau, v. 63, p. 773–786, doi:10.1007/BF01820841

Stump, E., 1981, Structural relationships in the Duncan Mountains, central Transantarctic Mountains, Antarctica: New Zealand Journal of Geology and Geophysics, v. 24, p. 87–93, doi:10.1080/00288306.1981.10422699

Stump, E., 1982, The Ross Supergroup in the Queen Maud Mountains, in Craddock, C., ed., Antarctic Geoscience: University of Wisconsin Press, Madison, WI; p. 565–569

Stump, E., 1986, Stratigraphy of the Ross Supergroup, Central Transantarctic Mountains, *in* Turner, M.D., and Splettstoesser, J.E., eds., Geology of the Central Transantarctic Mountains: American Geophysical Union, Antarctic Research Series, , v. 36, p. 225-274, doi:10.1029/AR036p0225

Stump, E., 1992, The Ross orogen of the Transantarctic Mountains in light of the Laurentia-Gondwana split: GSA Today, v. 2, p. 25–31.

Stump, E., 1995, The Ross orogen of the Transantarctic Mountains: Cambridge, Cambridge University Press, 308 p.

Stump, E., Gehrels, G., Talarico, F., and Carosi, R., 2007, Constraints from detrital zircon geochronology on the early deformation of the Ross orogen, Transantarctic mountains, Antarctica, *in* Cooper, A.K., and Raymond, C.R., eds., Antarctica: A Keystone in a Changing World – Online Proceedings of the 10th ISAES, USGS Open-File Report 2007-1047, Extended Abstract 166: 3 p.

Stump, E., Gootee, B., and Talarico, F., 2006, Tectonic model for development of the Byrd Glacier Discontinuity and surrounding regions of the Transantarctic Mountains during the Neoproterozoic-early Paleozoic, *in* Futterer, D., Damaske, D., Kleinschmidt, G., Miller, H., and Tessensohn, F., eds., Antarctica: Contributions to Global Earth Sciences: Berlin, Heidelberg, New York; Springer, p. 181–190.

Stump, E., Gootee, B.F., Talarico, F., Van Schmus, W.R., Brand, P. K., Foland, K.A., and Fanning, C.M., 2004, Correlation of Byrd and Selborne groups, with implications for the Byrd Glacier discontinuity, central Transantarctic Mountains, Antarctica: New Zealand Journal of Geology and Geophysics, v. 47, p. 157–171, doi:10.1080/00288306.2004.9515045

Talarico, F.M., Stump, E., Gootee, B.F., Foland, K.A., Palmeri, R., Van Schmus, W.R., Brand, P.K., and Ricci, C.A., 2007, First evidence of a "Barrovian"-type metamorphic regime in the Ross orogen of the Byrd Glacier area, central Transantarctic Mountains: Antarctic Science, v. 19, p. 451–470, doi:10.1017/S0954102007000594

Van Schmus, W.R., McKenna, L.W., Gonzales, D.A., Fetter, A.H., and Rowell, A.J., 1997, U-Pb geochronology of parts of the Pensacola, Thiel, and Queen Maud mountains, Antarctica, *in* Ricci, C.A., ed., The Antarctic Region: Geological Evolution and Processes: Siena, Italy; Terra Antarctica Publication, p. 187–200.

Vermeesch, P., 2012, On the visualisation of detrital age distributions: Chemical Geology, v. 312–313, p. 190–194, doi:10.1016/j.chemgeo.2012.04.021

Vogel, M.B., Ireland, T.R., and Weaver, S.D., 2002, The multistage history of the Queen Maud Batholith, La Gorce Mountains, central Transantarctic Mountains, *in* Gamble, J.A., Skinner, D. N.B., and Henrys, S.A., eds., Antarctica at the Close of a Millennium: Proceedings of the 8th International Symposium on Antarctic Earth Sciences: Wellington, New Zealand; Royal Society of New Zealand, p. 153–159.

Wade, F.A., and Cathey, C.A., 1986, Geology of the basement complex, Western Queen Maud Mountains, Antarctica, *in* Turner, M.D., and Splettstoesser, J.E., eds., Geology of the Central Transantarctic Mountains: American Geophysical Union, Antarctic Research Series, v. 36, p. 429-453.

Wareham, C.D., Stump, E., Storey, B.C., Millar, I.L., and Riley, T.R., 2001, Petrogenesis of the Cambrian Liv Group, a bimodal volcanic rock suite from the Ross orogen, Transantarctic Mountains: Geological Society of America Bulletin, v. 113, p. 360–372, doi:10.1130/0016-7606(2001)113<0360:POTCLG>2.0.CO;2

Warren, G., 1969, Geology of the Terra Nova Bay-McMurdo Sound area, Victoria Land: American Geographical Society. Antarctic Map Folio Series (folio 12, plate 13), scale 1:1,000,000.

York, D., Hall, C.M., Yanase, Y., Hanes, J.A., and Kenyon, W.J., 1981, $^{40}Ar/^{39}Ar$ dating of terrestrial minerals with a continuous laser: Geophysical Research Letters, v. 8, p. 1136–1138, doi:10.1029/GL008i011p01136